THE ASTROPHYSICAL JOURNAL, 394:228–247, 1992 July 20

A SPECTROSCOPIC DETERMINATION OF THE MASS DISTRIBUTION OF DA WHITE DWARFS

P. BERGERON,[1,2] REX A. SAFFER,[1,3] AND JAMES LIEBERT[1]

Received 1991 December 9; accepted 1992 January 30

ABSTRACT

A mass distribution for a sample of 129 DA white dwarfs is presented, based on fitting hydrogen line profiles to the predictions of stellar atmosphere models. The atmospheric parameters determined from spectroscopy are shown to be of improved accuracy over those obtained with other techniques. The spectroscopic masses are in good agreement with those inferred from gravitational redshift measurements. The comparison includes objects of particular astrophysical interest such as the Pleiades white dwarf LB 1497 (0.98 $M_\odot$), and 40 Eri B (0.51 $M_\odot$). The masses obtained for the stars in the Hyades cluster are found to be measurably higher than those of field stars. The surface gravities obtained from spectroscopy are also consistent with those obtained from trigonometric parallaxes although the observed scatter is greatly reduced in the spectroscopic analysis. The observed mass distribution exhibits a narrow peak, but broad and flat tails extend to large and small masses. The mean mass of the distribution is somewhat lower—near 0.56 $M_\odot$—than found in the best previous analyses. The mode of the distribution is in the narrow mass range 0.50–0.55 $M_\odot$, which contains more than 30% of the stars observed, and the median has a value of $M = 0.54\ M_\odot$. Nearly 10% of the stars have masses low enough that their existence must be ascribed to close binary evolution. Zuckerman & Becklin have found recently that two of those objects have low-mass nondegenerate companions. The high-mass tail includes one object (GD 50) near 1.3 $M_\odot$. The consequences of these results for earlier phases of stellar evolution are discussed.

Subject headings: stars: fundamental parameters — stars: luminosity function, mass function — white dwarfs

1. INTRODUCTION

The distributions of white dwarf parameters, such as effective temperatures and masses, can reveal important constraints for earlier phases of stellar evolution and for the history of the Galactic disk population. The complete history of star formation in the disk can be reconstructed, in principle, if both the luminosity function and the mass distribution of the degenerate stars can be determined accurately, and if the relationship between the initial and final mass of a star is understood in detail. It is the mass distribution which is the exclusive topic of the analysis presented here, although it is restricted to the majority of white dwarfs which have atmospheric compositions dominated by hydrogen (DA spectral type). In the remainder of this section, the methods used in determining the masses of DA stars are discussed, and the most important previous determinations of the mass distribution are reviewed.

1.1. *Methods for Determining White Dwarf Masses*

There are several ways in which the masses of white dwarfs may be estimated. First, there are several in wide binary systems with masses determined directly from the orbital solution. The only apparently well-studied cases, however, yield much different values: 40 Eri B at 0.43 $M_\odot$ (Heintz 1974), and Sirius B at 1.05 $M_\odot$ (Gatewood & Gatewood 1978). Procyon B, near 0.65 $M_\odot$, does not even have a reliable spectral classification, while the cool DC star Stein 2051B has traversed only a fraction of one orbital period in available photography. Several other white dwarfs are in binary systems so close that their evolution and the resulting masses may have been affected by mass exchange.

A second, very promising method for direct mass determinations of white dwarfs is discussed by Kawaler (1991): the masses derived from pulsational mode analysis. Although pulsating white dwarfs include both DA and DB stars in restricted ranges of effective temperatures this method is applicable currently only to the very hot, pre–white dwarf objects of the PG 1159−035 (GW Vir) class (Winget et al. 1991; Fontaine et al. 1991).

A third path to the estimation of white dwarf masses involves the direct measurement of the gravitational redshift, the ratio of the mass to the radius (see Wegner 1989 for a review). One then needs a second relationship between mass and radius, or an independent determination of the radius. For example, one can employ a theoretical mass-radius relation for the appropriate composition such as those calculated by Hamada & Salpeter (1961) for zero-temperature degenerate configurations. Better still is the use of evolutionary models in which finite-temperature effects on the radius are considered. Alternatively, the radius may be estimated by one of the methods discussed below. The gravitational redshift method cannot be applied easily to a large sample of stars, however, since one needs to know also the star's intrinsic radial velocity—the true motion toward or away from the Sun. Its use has been largely restricted to DA white dwarfs which have relatively sharp Hα and Hβ line cores. A few dozen white dwarfs are directly useful since they have common proper motion companions or are members of a star cluster or moving group (Koester 1987; Wegner 1989; Wegner & Reid 1991).

For a fourth group of white dwarfs—those for which accurate trigonometric parallax measurements are available—the radius may be estimated with minimal application of stellar atmospheres theory. One takes only the effective temperature

[1] Steward Observatory, University of Arizona, Tucson, AZ 85721

[2] Current postal address: Département de Physique, Université de Montréal, C. P. 6128, Succ. A, Montréal, Québec, Canada, H3C 3J7

[3] Current postal address: Space Telescope Science Institute, 3700 San Martin Drive, Baltimore, MD 21218

estimate (T_{eff}) from a model fit to observational data, combined with a luminosity (L) obtained primarily from the distance measurement, to determine the radius. The combination of this with a theoretical mass-radius relation yields an estimate of the white dwarf mass. Koester, Schulz, & Weidemann (1979, hereafter KSW) define masses obtained from radii in this way as the $M(R)$ distribution. Accurate parallaxes need to be large, so that nearer, cooler, often non–DA white dwarfs dominate the sample optimum for this method. Several dozen hot DA stars have published trigonometric parallaxes, but for most of these the error in the parallax is significant compared with the measurement. If the measured trigonometric values are systematically too large or too small by modest amounts, the $M(R)$ analysis may be subject to a corresponding systematic error.

The fifth and most general method is a full comparison of properties of the observed spectrum with predictions of stellar atmosphere models in order to estimate the surface gravity as well as the effective temperature of the star, the $M(g)$ method. The former is, of course, the ratio of the mass to the square of the radius and may be combined with a theoretical mass-radius relation to yield the stellar mass. One may apply this method to large samples including those defined from kinematically unbiased color surveys such as the Palomar Green (Green, Schmidt, & Liebert 1986), Kitt Peak Downes (Downes 1986), or the Montréal Cambridge Tololo (Demers et al. 1987). The method is most suitable for DA white dwarfs since the physics of hydrogen-rich atmospheres is generally better understood than for the hydrogen-poor counterparts; consequently, the discussion will be restricted to DA white dwarfs.

1.2. *Previous Estimates of DA White Dwarf Masses*

The most comprehensive analyses of large samples of DA white dwarfs have used photometric data, the best of which are Strömgren and Palomar multichannel (MCSP; Greenstein 1984) colors. Both include a color index which is sensitive to the surface gravity by measuring the strength of the Balmer jump; this may be plotted against color indices like the Greenstein $(g-r)$ or the Strömgren $(b-y)$ which measure the Paschen-continuum slope and are therefore sensitive primarily to effective temperature. These analyses include those of KSW, Wegner (1979), Shipman & Sass (1980), Weidemann & Koester (1984, hereafter WK), and Fontaine et al. (1985). McMahan (1989) fitted low-resolution optical spectrophotometry to synthetic spectra predicted by models. Alternatively, Shipman (1979), KSW, and McMahan (1989) have used the trigonometric parallax technique to measure directly the stellar radius.

The accuracies of these analyses were severely limited by both observational and systematic errors with the data. First of all, Strömgren photometry uses bandpasses of only several hundred Å, requiring long integration times on telescopes of moderate (1–1.5 m) aperture to achieve even moderate photon statistics of a few percent. Moreover, due to variations primarily in Strömgren filter sets, systematic differences became evident in colors measured by different observers. Likewise, the Palomar 5 m MCSP colors, despite the relative abundance of photons, were limited by the accuracy with which mean atmospheric extinctions were obtained, the relatively modest entrance apertures, and the manner in which spectrophotometric standardization was performed. Both sets of colors faced systematic uncertainties based on how the spectrophotometry was tied to the true fluxes of Vega. For example, in the analysis of WK, the mean mass is shifted by 0.04 $M_\odot$ depending on whether the absolute calibration of Oke & Gunn (1983; AB79) or that of Hayes & Latham (1975) was used for the MCSP colors.

The mean masses and distributions derived for such samples show a tendency to depend on the range of T_{eff} used. In particular, inspection of the relevant figures shows that the mean mass would have been lower in KSW's investigation had they restricted their analysis to effective temperatures higher than $T_{eff} = 13{,}000$ K. The temperature dependence of the result for Strömgren colors led Wegner (1979) to "adjust" the theoretical curves of constant log g so that they followed the data points! The most pronounced temperature dependence may appear in the analysis of Shipman & Sass (1980), although this has been explained by the way theoretical colors were transformed from the MCSP to the Strömgren system (Fontaine et al. 1985).

Despite the inhomogeneous nature of the previous investigations, these analyses of DA stars have produced surprisingly similar and consistent results. KSW found from trigonometric parallax analyses a mean radius of log $R/R_\odot = -1.920$ with a very narrow dispersion of $\sigma = 0.093$. This corresponds to a mass of $M = 0.602$ $M_\odot$ using the mass-radius relation of Hamada & Salpeter (1961)[4]. Their result is consistent with the analysis of Shipman (1979) who found a mean radius of log $R/R_\odot = -1.896$. KSW have also used photometric techniques to determine a mean surface gravity of log $g = 7.926$, or $M = 0.522$ $M_\odot$, using the Hayes & Latham (1975) calibration, with a dispersion of $\sigma(\log g) = 0.285$. The result based on the Tüg, White, & Lockwood (1977) calibration yields a higher mean surface gravity of log $g = 8.092$, or $M = 0.624$ $M_\odot$, with a comparable dispersion. As discussed by KSW, the Tüg et al. calibration leads to very high values of log g at the hot and cool ends of their observed sequence, and therefore, the former calibration was preferred. When the surface gravity of each star is converted into mass before taking the average, the analysis yields a mean mass of $M = 0.535$ $M_\odot$ with a dispersion of only $\sigma(M) = 0.155$ $M_\odot$. The dispersion is further reduced to 0.138 $M_\odot$ if the analysis is restricted to the parallax ensemble which is intrinsically brighter, and therefore of better quality.

WK improved the results of KSW by using a more homogeneous data set (MCSP data), and by restricting their analysis to a range of effective temperature where the sensitivity of color indices to surface gravity is the largest ($8000 \lesssim T_{eff} \lesssim 16{,}000$ K). The analysis has produced what is probably the best determination of the mass distribution of DA stars to date. The mass distribution shows a steep increase at ~ 0.45 $M_\odot$ with an extended tail at high masses. The average mass is $M = 0.58$ $M_\odot$ with a dispersion of $\sigma(M) = 0.13$ $M_\odot$ using the preferred Hayes-Latham calibration, or $M = 0.62$ $M_\odot$ using the AB79 color calibration. The corresponding log g analysis yields an average value of log $g = 8.02$ with a dispersion of $\sigma(\log g) = 0.22$.

The most recent analysis is that of McMahan (1989). His unweighted mean mass is $M = 0.546$ $M_\odot$ with a dispersion of $\sigma(M) = 0.192$, or $M = 0.480$ $M_\odot$ with a dispersion of $\sigma(M) = 0.014$ for the weighted average. These values are significantly different from previous determinations, especially the

[4] The mass quoted in the abstract of KSW is 0.58 $M_\odot$, although our own derivation of the mass corresponding to an average radius of log $R/R_\odot = -1.920$ is $M = 0.602$ $M_\odot$ using the mass-radius relation of Hamada-Salpeter for carbon-core configurations. Similarly, the numbers quoted at the bottom left of p. 272 of KSW should read 0.602 and 0.612 $M_\odot$.

weighted average, although his result of the mean radius determined from trigonometric parallax (log $R/R_{\odot} = -1.905$, $\sigma = 0.087$) is in excellent agreement with other analysis. The mass distributions obtained by McMahan (1989) and WK are discussed further in § 5. Note that all of these results were obtained using the zero-temperature Hamada-Salpeter relation, which we shall show later can result in significant underestimates of the masses.

1.3. *Physical Uncertainties Associated with Previous Analyses*

The samples of white dwarfs used in previous analyses are dominated or influenced heavily by stars below $T_{\rm eff} \sim 15{,}000$ K, where the color indices are most sensitive to surface gravity, and also because the bulk of DA white dwarfs is found in this range of temperatures. However, as discussed below, the model atmospheres in this particular region are very sensitive to the input physics and the assumed atmospheric composition, and previous estimates of atmospheric parameters of white dwarfs may need to be reconsidered.

In cool ($T_{\rm eff} \lesssim 12{,}000$ K) DA stars, large amount of helium can be brought to the surface by convection while still remaining spectroscopically invisible. Bergeron, Wesemael, & Fontaine (1991d) have shown (see their Fig. 17) that the effect on the predicted colors of an increase in surface gravity in such stars, as measured by the strength of the Balmer jump, can also be reproduced by increasing the helium abundance, as also noticed by Wegner & Schulz (1981). It is clear that in such color-color diagrams, massive DA white dwarfs with pure hydrogen atmospheres could just as well be interpreted as helium-enriched objects with normal masses. A detailed analysis of the high Balmer line profiles lead to similar conclusions. Therefore, Bergeron et al. (1991d) conclude that, on the basis of optical spectroscopy and photometry, it is not possible to separate the pressure effects originating from an increased helium abundance from those stemming from an increased surface gravity.[5] These results bear profound implications for previous determinations of the mass (or surface gravity) distribution of cool DA stars.

Below $T_{\rm eff} \sim 15{,}000$ K, the atmospheres of DA white dwarfs become convective. Model atmospheres for these stars are usually calculated using the standard mixing-length theory, with a value of $l/H = 1$ (the so-called ML1 version of the mixing-length theory). However, as discussed by Fontaine, Tassoul, & Wesemael (1984), the efficiency of convection needs to be increased significantly in order to explain the observed location of the blue edge of the ZZ Ceti instability strip. Recently, Bergeron, Wesemael, & Fontaine (1992) have carried out a series of model atmosphere calculations which are used to study the influence of the convective efficiency on the determination of the atmospheric parameters of DA white dwarfs (see also Wesemael et al. 1991). Their results show that the predicted emergent fluxes, color indices, and equivalent widths are most sensitive to the assumed parameterization of the convection theory in the range $T_{\rm eff} \sim 8000$–$15{,}000$ K. It is therefore concluded that previous determinations of the mass distribution using photometric, spectroscopic, or even trigonometric parallax techniques in this range of effective temperature should be considered model-dependent. In particular, the analysis of the morphology of color-color diagrams reveals that the *absolute value* of the mean surface gravity depends strongly on the assumed convective efficiency.

Above $T_{\rm eff} \sim 15{,}000$ K, the atmospheres of DA stars are completely radiative and thus do not suffer from the uncertainties in convection theory discussed above. Furthermore, the absence of convection ensures that the chemical separation in the atmospheric regions by gravitational settling is maintained, leading to a hydrogen-rich atmospheric composition. Therefore, the uncertainties in the input physics and/or atmospheric compositions are minimized. Unfortunately, because of the gradual disappearance of the Balmer jump at high effective temperature, photometric analyses become rapidly insensitive to surface gravity above $T_{\rm eff} \sim 20{,}000$ K (see e.g., KSW). Furthermore, the errors of the measured parallax are larger than those associated with the cooler stars since the hot white dwarfs are intrinsically brighter, and therefore farther away.

As discussed below, however, the profiles of Balmer lines are still very sensitive to surface gravity variations, even at these high effective temperatures. With these considerations in mind, the spectroscopic technique of fitting detailed hydrogen line profiles has been applied to a large sample of DA stars with radiative, hydrogen-rich atmospheres. The results of this investigation are reported here. In § 2, the selection of the sample and the spectroscopic observations are described. The fitting technique and the results of the analysis are presented in § 3. In § 4, the masses determined from spectroscopy are then tested against masses inferred from gravitational redshift measurements, and trigonometric parallaxes. The mass distribution and its implications for stellar and Galactic evolution are presented in § 5. Several objects of particular astrophysical interest are discussed in § 6, and the conclusions follow in § 7. Preliminary reports of this work while still in progress appear in Bergeron, Saffer, & Liebert (1991b, c). The numerical values given in these conference proceedings are superseded by those presented here.

2. SPECTROSCOPIC OBSERVATIONS

The sample of DA white dwarfs studied in this analysis has been drawn from the catalog of spectroscopically identified white dwarfs of McCook & Sion (1987). Most objects have been selected with spectral types DA2 and DA3, which correspond approximately to effective temperatures in the range 15,000–30,000 K where atmospheric convection is negligible. Four stars (40 Eri B, G148-7, Wolf 485A, and G142-B2A) with spectral types DA4 for which masses estimated from gravitational redshifts are available were included in the sample as well. Several stars observed in the sample turned out to have either the wrong spectral classification, or some other particular feature, and were therefore withdrawn from the analysis: PG 0111+177, PG 0221+217, PG 0319+055, PG 0910+622, PG 0933+383, PG 0947+639, PG 1236+479, PG 1430+427, PG 1549+001,[6] GD 354, and PG 2128+113 are low-gravity objects, most of which are subdwarf B stars (Saffer et al. 1992a); GD 561 is a hot DAO star with He II λ4686 clearly visible; HZ 9 is a precataclysmic binary (Lanning & Pesch 1981) which could not be analyzed properly because the DA

[5] Note that this result does *not* depend on the conclusions of Bergeron et al. (1990) who showed that in order to fit the line profiles of their sample of 37 cool DA stars with pure hydrogen models, the mean surface gravity had to be increased to log $g \sim 8.2$ (a similar conccusion was reached by Dolez, Vauclair, & Koester 1991). They attributed this high value of the mean surface gravity to the presence of helium in the atmospheres of most cool DA stars.

[6] The declination of PG 1549+001 should read +00 04 16 (1950.0) instead of −00 04 16 as reported in the Palomar-Green catalog.

TABLE 1

ATMOSPHERIC PARAMETERS FOR DA WHITE DWARFS

WD	Name	V	$T_{\rm eff}$(K)	log g	$M/M_\odot$	M_V	Notes
0048+202........	PG 0048+202	15.84	20340	7.97	0.58	10.76	
0058−044........	GD 9	15.38	16630	8.00	0.59	11.15	1
0102+095........	PHL 972	14.46	25290	7.91	0.56	10.27	
0103−278........	G269-93	15.45	12970	8.00	0.58	11.62	
0106+372........	GD 11	15.25	29730	7.78	0.50	9.73	
0126+422........	GD 13	14.95	22410	7.81	0.50	10.36	
0127+270........	GD 14	16.20	25630	7.77	0.49	10.04	
0134+833........	GD 419	13.08	18730	8.07	0.64	11.05	2
0136+768........	GD 420	15.04	16250	7.71	0.44	10.80	
0147+674........	GD 421	14.42	30710	7.63	0.45	9.43	
0148+467........	GD 279	12.44	13990	7.89	0.53	11.32	2
0205+551........	GD 282	15.89	16660	7.95	0.56	11.08	
0214+568........	H Per 1166	13.68	21180	7.83	0.51	10.50	
0216+143........	PG 0216+144	14.51	27680	7.80	0.51	9.92	
0227+050........	Feige 22	12.83	19070	7.78	0.48	10.61	3
0229+270........	LP 354-382	15.58	24540	7.88	0.54	10.29	
0232+525........	G174-5	13.75	17050	8.26	0.75	11.49	3
0259+378........	GD 38	15.55	31730	7.72	0.48	9.49	
0302+028........	GD 41	14.80	35830	7.79	0.52	9.37	4
0312+223........	GD 43	15.85	18380	7.79	0.49	10.69	
0316+345........	GD 45	14.19	14880	7.61	0.40	10.83	
0339+523........	Rubin 70	15.80	13350	7.47	0.34	10.84	
0339−035........	GD 47	15.20	14620	7.90	0.53	11.25	
0346−011........	GD 50	13.98	40540	9.22	1.27	11.81	2
0349+247........	LB 1497	16.52	32920	8.60	0.98	10.83	3, 5, 6
0408−041........	GD 56	15.50	15000	8.01	0.60	11.36	
0410+117........	HZ 2	13.86	20790	7.94	0.56	10.68	2, 3
0413−077........	40 Eri B	9.52	16400	7.85	0.51	10.98	1, 3, 6
0421+162........	GH 7-191	14.29	18960	8.00	0.60	10.93	3, 6, 7
0425+168........	GH 7-233	14.02	23800	8.06	0.64	10.61	3, 6, 7
0431+125........	HZ 7	14.18	21150	8.05	0.63	10.81	3, 6, 7
0438+108........	HZ 14	13.83	27230	8.05	0.64	10.33	2, 3, 6, 7
0453+418........	GD 64	14.00	14260	7.71	0.43	11.03	2
0612+177........	G104-27	13.39	24660	7.94	0.57	10.37	3
0625+415........	GD 74	14.99	16910	7.99	0.59	11.11	
0644+375........	G87-7	12.07	21060	8.10	0.66	10.89	3
0710+741........	GD 448	14.97	18930	7.45	0.35	10.15	
0730+487........	GD 86	14.96	15510	8.49	0.90	12.03	
0817+386........	PG 0817+386	15.89	25930	8.00	0.61	10.37	
0839+231........	PG 0839+232	14.65	25070	7.74	0.48	10.04	
0854+404........	GD 98	14.90	22540	7.88	0.54	10.45	
0947+325........	Ton 458	15.38	22230	8.29	0.78	11.09	
1003−023........	PG 1003−023	15.43	20180	7.91	0.55	10.69	
1005+642........	GD 462	14.03	19770	7.92	0.55	10.74	
1015+161........	PG 1015+161	15.57	19800	8.07	0.64	10.95	
1019+129........	PG 1019+129	15.03	18320	7.97	0.58	10.94	
1034+492........	GD 304	15.41	20780	8.11	0.66	10.93	
1038+633........	PG 1038+634	15.49	24800	8.39	0.85	11.05	
1039+747........	PG 1039+748	15.61	29810	7.64	0.45	9.52	
1041+580........	PG 1041+580	14.59	30630	7.77	0.51	9.66	
1052+273........	GD 125	14.12	22750	8.41	0.86	11.24	3
1101+364........	PG 1101+364	14.44	13610	7.38	0.31	10.66	
1102+748........	GD 466	14.97	19800	8.37	0.83	11.41	
1104+602........	G197-4	13.80	18220	8.04	0.62	11.05	3
1105−048........	G163-50	12.92	15540	7.82	0.49	11.03	1, 3, 6
1113+413........	PG 1113+413	15.57	25870	7.82	0.52	10.10	
1125−025........	PG 1125−026	15.32	31410	8.18	0.72	10.21	
1126+384........	GD 310	14.73	25460	7.92	0.56	10.28	3
1133+293........	Feige 45	15.00	23460	7.80	0.50	10.26	
1134+300........	GD 140	12.50	21690	8.48	0.90	11.44	2, 3

TABLE 1—*Continued*

WD	Name	V	T_{eff}(K)	log g	$M/M_{\odot}$	M_V	Notes
1143+321........	G148-7	13.65	15360	7.99	0.58	11.28	2, 3, 6
1145+187........	PG 1145+188	14.18	27240	7.77	0.50	9.92	
1201−001........	PG 1201−001	15.12	19960	8.26	0.75	11.22	
1202+308........	Ton 75	15.00	29120	7.78	0.50	9.78	
1204+450........	PG 1204+451	14.84	23000	7.75	0.48	10.23	
1232+479........	GD 148	14.52	14700	7.90	0.53	11.23	
1241+010........	PG 1241−010	14.02	24010	7.22	0.31	9.32	
1249+182........	GD 151	15.48	19910	7.76	0.47	10.50	
1257+032........	PB 4421	15.60	17520	7.73	0.46	10.69	
1257+047........	GD 267	14.99	22310	7.93	0.56	10.55	
1301+544........	PG 1301+545	15.51	34020	8.03	0.64	9.84	
1305+018........	PG 1305+018	15.16	29430	7.82	0.52	9.82	
1317+453........	G177-31	14.13	14000	7.43	0.33	10.69	3
1319+466........	G177-34	14.55	14640	8.18	0.70	11.65	
1327−083........	Wolf 485A	12.30	14350	7.92	0.54	11.31	2, 3, 6
1330+473........	PG 1330+473	15.29	22570	7.89	0.54	10.46	
1333+497........	PG 1333+498	15.30	29850	7.97	0.60	10.02	
1334−160........	L762-21	15.35	18990	8.32	0.80	11.41	6
1335+700........	PG 1335+701	15.33	30530	8.23	0.75	10.35	
1337+705........	G238-44	12.79	20230	7.90	0.55	10.68	3
1344+572........	G223-24	13.30	14060	7.96	0.56	11.40	
1353+409........	PB 999	15.43	23580	7.54	0.40	9.88	
1408+323........	GD 163	13.97	18410	7.97	0.58	10.94	2, 3
1421+318........	Ton 197	15.30	27620	7.97	0.59	10.18	
1446+286........	Ton 214	14.54	22940	8.36	0.82	11.14	
1449+168........	PG 1449+168	15.39	21510	7.87	0.53	10.52	
1451+006........	GD 173	15.29	25670	7.83	0.52	10.14	
1459+305........	PG 1459+306	13.98	26170	7.89	0.55	10.19	
1507+220........	PG 1507+220	15.00	19380	7.81	0.50	10.63	
1509+322........	GD 178	14.11	14660	8.00	0.59	11.39	3
1513+442........	PG 1513+442	15.41	29700	7.83	0.53	9.81	
1521+310........	Ton 229	15.05	26460	7.90	0.56	10.17	
1531−022........	GD 185	13.90	18870	8.39	0.84	11.53	
1548+149........	PG 1548+149	15.06	20800	7.84	0.51	10.54	
1553+353........	PG 1553+354	14.71	26220	7.80	0.51	10.04	
1554+215........	PG 1554+215	15.07	27220	7.87	0.54	10.07	
1608+118........	PG 1608+119	15.26	20460	7.91	0.55	10.66	
1609+044........	PG 1609+045	15.29	29720	7.90	0.56	9.91	
1614+136........	PG 1614+137	15.19	22430	7.34	0.33	9.65	
1615−154........	G153-41	13.42	29730	7.94	0.58	9.98	3
1647+375........	PG 1647+376	15.01	21750	7.89	0.54	10.52	
1713+332........	GD 360	14.46	22030	7.40	0.35	9.79	1
1713+695........	G240-51	13.27	15600	7.90	0.53	11.13	2, 3
1845+019........	Lanning 18	12.96	29840	7.78	0.51	9.73	
1911+135........	G142-B2A	14.00	13770	7.83	0.49	11.27	3, 6
1918+725........	GD 533	15.12	22350	7.88	0.54	10.46	
1936+327........	GD 222	13.58	21260	7.84	0.52	10.50	2
1943+163........	G142-50	13.99	19410	7.80	0.49	10.61	2
2009+622........	GD 543	15.15	25870	7.70	0.46	9.93	
2028+390........	GD 391	13.37	24630	7.87	0.54	10.27	2
2032+188........	GD 231	15.34	18540	7.48	0.36	10.24	2
2032+248........	G186-31	11.52	19980	7.83	0.51	10.60	3
2039−202........	L711-10	12.34	19900	7.93	0.56	10.75	3
2111+498........	GD 394	13.09	39450	7.83	0.55	9.30	2
2115+010........	PG 2115+011	15.60	25490	7.84	0.53	10.16	
2117+539........	G231-40	12.33	14490	7.85	0.50	11.19	1, 2, 3
2134+218........	GD 234	14.45	18310	8.07	0.64	11.09	
2136+828........	G261-45	13.02	16940	7.84	0.50	10.90	2, 3
2143+353........	GD 396	15.50	25630	7.84	0.52	10.14	
2149+021........	G93-48	12.77	18250	8.02	0.61	11.02	2, 3

TABLE 1—*Continued*

WD	Name	V	T_{eff}(K)	log g	$M/M_\odot$	M_V	Notes
2150+338........	GD 398	15.13	17890	7.87	0.52	10.85	
2204+071........	PG 2204+071	14.74	23570	7.93	0.56	10.44	
2226+061........	GD 236	14.72	15840	7.68	0.43	10.80	
2302+457........	GD 404	15.82	23540	7.90	0.55	10.40	
2319+691........	GD 559	14.61	19560	7.91	0.55	10.74	
2328+107........	PG 2328+108	15.55	23120	7.83	0.52	10.33	
2329+407........	G171-2	13.82	15900	7.91	0.54	11.11	2
2331+290........	GD 251	15.80	27830	7.50	0.39	9.47	
2336+063........	PB 5486	15.60	17000	8.01	0.60	11.13	

NOTES.—(1) Also observed by WK. (2) Also observed by McMahan 1989. (3) Also observed by KSW. (4) This star has been originally classified as a subdwarf B star in the Palomar-Green catalog. (5) Pleiades member. (6) Gravitational redshift object. (7) Hyades member.

absorption lines are diluted and have cores filled in with emission; LB 11146 is a star with a peculiar optical continuum and distorted line profiles. An independent analysis of the latter object is currently underway, the results of which will be reported elsewhere.

A sample of 129 DA stars north of decl. $\sim -30°$ has finally been retained for the analysis. These objects are listed in Table 1.[7] Particular care was taken to include the hottest four white dwarfs in the Hyades cluster, and also the one which is likely to be an evolved Pleiades member. The magnitudes given in Table 1 are either the Johnson V, the multichannel v, or the Strömgren y magnitudes. Figure 1 shows the distribution as a function of V (or equivalent) of all stars observed, and indicates that the sample is complete down to $V \sim 15.5$, although fainter objects have been included in the sample as well.

[7] GD 41 (PG 0302+028) has been misclassified as a subdwarf B star in the PG catalog, but is really a DA2 (Saffer et al. 1992a). Also, in the McCook & Sion catalog, WD 1104+602 and WD 1100+604 are the same object (G197-4). Three more objects (SA 51-822A, L817-13, and L825-14) had no finding charts available.

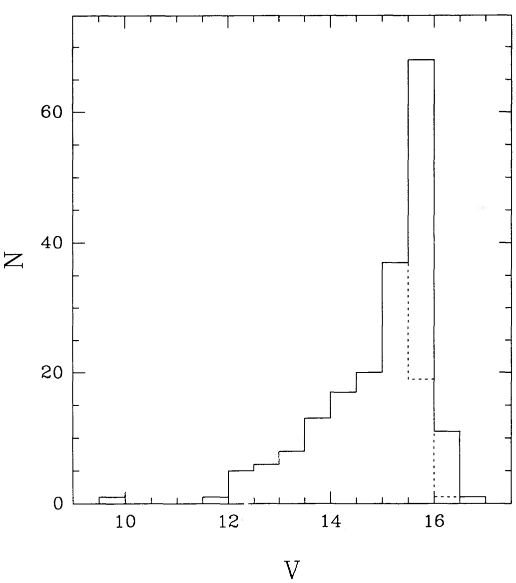

FIG. 1.—Distribution of DA stars as a function of the magnitude V. The solid line indicates the distribution of all objects found in the McCook & Sion catalog with spectral types DA2 and DA3 (including the gravitational redshift objects discussed in § 2) north of decl. $\sim -30°$. The dashed line shows the distribution of the 129 DA stars selected and observed in the final analysis.

Optical spectroscopy has been obtained for each object listed in Table 1 using the Steward Observatory 2.3 m reflector telescope equipped with the Boller & Chivens spectrograph and a UV-flooded Texas Instrument CCD detector. The 4".5 slit together with the 600 lines mm^{-1} grating blazed at λ3568 in first order provided a spectral coverage of $\lambda\lambda$3750–5100 at an intermediate resolution of $\sim$6 Å FWHM. High signal-to-noise ratio (S/N > 80) spectroscopy was obtained for each star; such a high S/N is required to make precise determination of atmospheric parameters. Further details on the observing and reduction procedure can be found in Saffer et al. (1992a). The complete sample of optical spectra which serves as the basis of this analysis is presented in Figure 2.

3. THE SPECTROSCOPIC TECHNIQUE

3.1. *Synthetic Spectra*

The observed line profiles contain a wealth of information about the effective temperature and surface gravity (see, e.g., Schulz & Wegner 1981). In particular, the profiles of all Balmer lines are quite sensitive to T_{eff} variations, as well as log g variations, in this case due to linear Stark broadening that follows variations in the atmospheric pressure. In order to make successful use of analyses of the high Balmer lines, however, a detailed knowledge is required of how the high-lying levels of the hydrogen atom are perturbed. Such a treatment has been developed by Hummer & Mihalas (1988), in which the atomic level populations are calculated within an occupation probability formalism. This formalism provides an improved theoretical framework which permits a careful analysis of the gravity-sensitive high Balmer lines in DA stars. The application of the Hummer-Mihalas formalism in the context of white dwarf atmosphere is discussed at length in Bergeron et al. (1991d). Spectroscopic analyses of samples of ZZ Ceti and cool DA stars using this new generation of synthetic spectra are presented in Bergeron et al. (1990) and Daou et al. (1990).

The models used here differ slightly from those used in previous analyses: New Stark broadening profiles for the complete Balmer line series have been kindly provided by T. Schöning and K. Butler. These profiles are calculated following the prescription of Vidal, Cooper, & Smith (1970) in which reference the profiles for only the first four Balmer lines were tabulated. In addition, the occupation probabilities have been calculated allowing for particle correlation in the microfield distribution. With these models, systematic differences were found between the atmospheric parameters obtained from

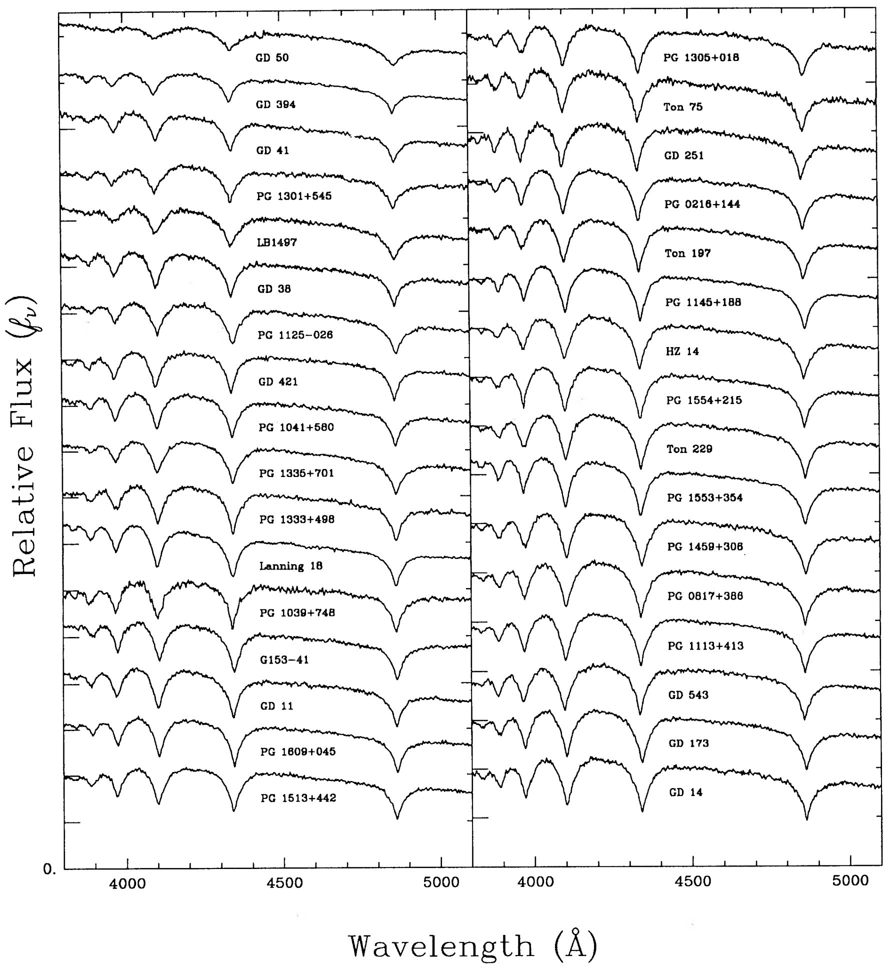

FIG. 2*a*

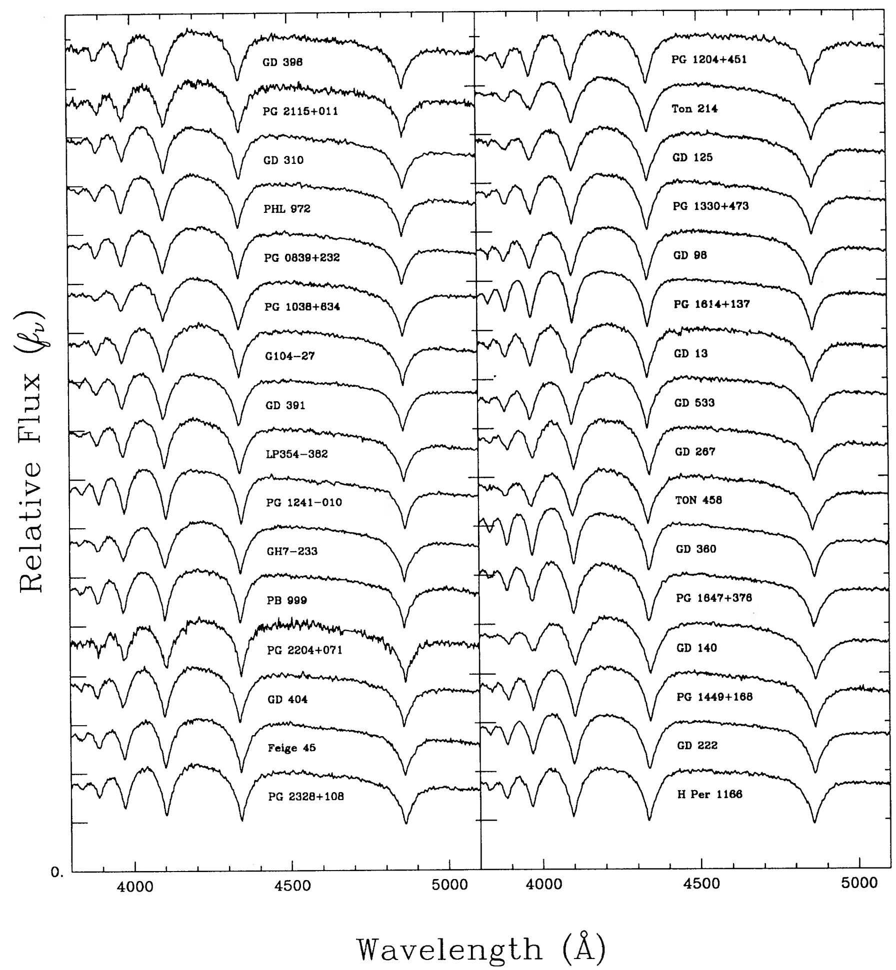

FIG. 2*b*

FIG. 2.—Optical spectra for the complete sample of DA stars. The spectra are normalized at 4500 Å and are shifted vertically; the various zero points are indicated by long tick marks. The effective temperature decreases from upper left to bottom right.

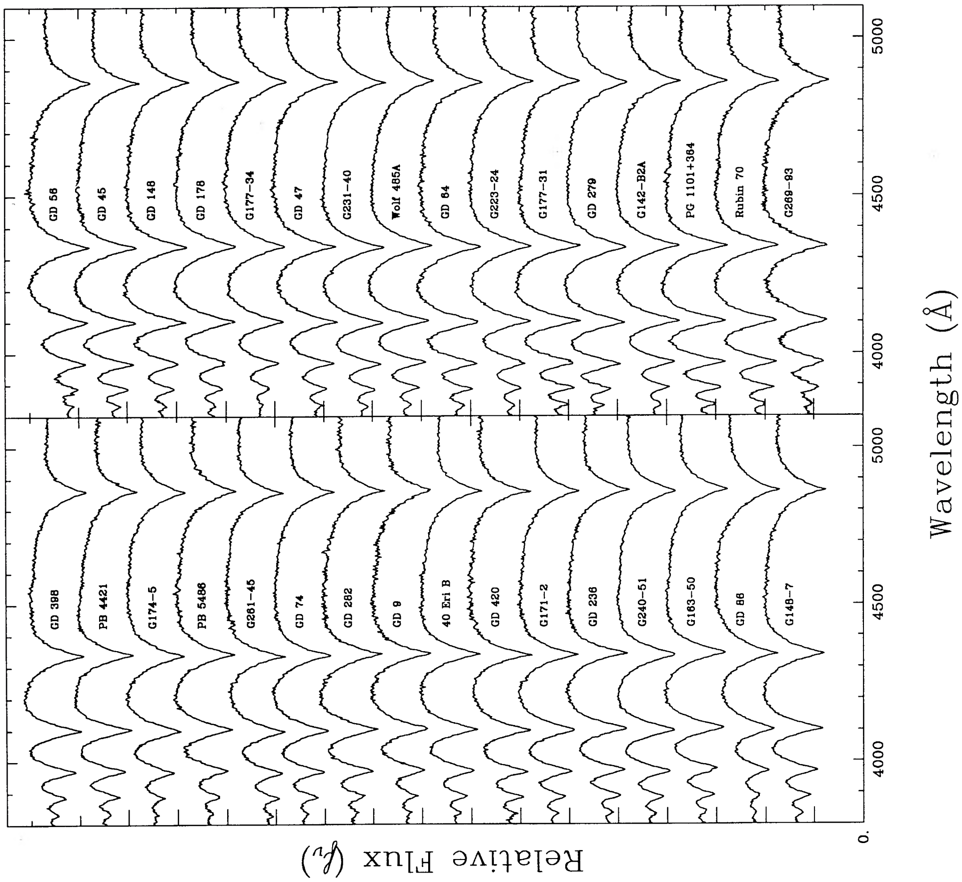
GD 398
PB 4421
G174-5
PB 5486
G281-45
GD 74
GD 282
GD 9
40 Eri B
GD 420
G171-2
GD 236
G240-51
G163-50
GD 86
G148-7
GD 56
GD 45
GD 148
GD 178
G177-34
GD 47
G231-40
Wolf 485A
GD 64
G223-24
G177-31
GD 279
G142-B2A
PG 1101+364
Rubin 70
G269-93
4000
4500
5000
0.
Wavelength (Å)
Relative Flux (f_ν)

FIG. 2d

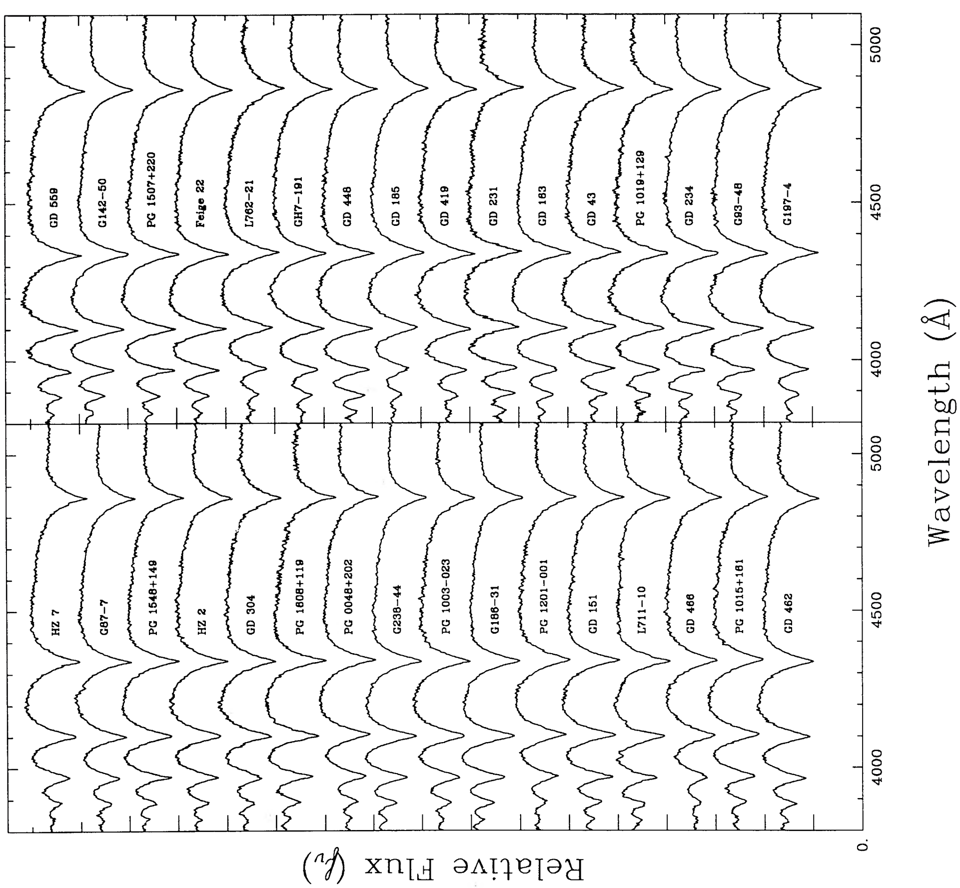
HZ 7
G87-7
PG 1548+149
HZ 2
GD 304
PG 1608+119
PG 0048+202
G238-44
PG 1003-023
G186-31
PG 1201-001
GD 151
L711-10
GD 486
PG 1015+161
GD 462
GD 559
G142-50
PG 1507+220
Feige 22
L762-21
GH7-191
GD 448
GD 185
GD 419
GD 231
GD 183
GD 43
PG 1019+129
GD 234
G93-48
G197-4
4000
4500
5000
0.
Wavelength (Å)
Relative Flux (f_ν)

FIG. 2c

individual Balmer lines. This discrepancy was removed by adjusting the value of the microfield until all lines yield consistent solutions. With this approach, it was also possible to match the laboratory data such as those analyzed by Seaton (1990). A more detailed discussion of these problems will be presented elsewhere. These refinements of the theoretical models were only partially included in the preliminary analyses reported in Bergeron et al. (1991b, c).

The LTE model atmospheres used are similar to those described by Wesemael et al. (1980), which are hydrogen-line blanketed and assume a pure hydrogen composition. The thermodynamic stratifications of these models are then used to calculate detailed emergent fluxes and line profiles. Theoretical line profiles have been calculated for a range of atmospheric parameters of $T_{\rm eff} = 12{,}000$ (1000) 45,000 K, and $\log g = 7.0$ (0.25) 9.0 (a small subset of models at $\log g = 9.5$ has also been calculated to fit the most massive objects in the sample).

Although the sensitivity of photometric techniques to surface gravity decreases rapidly for effective temperatures above $\sim$20,000 K, the Balmer line profiles are still very sensitive to variations of $\log g$ at higher effective temperatures, as illustrated in Figure 3. In these models, the equivalent widths of the lower Balmer lines (Hβ and Hγ) increase with increasing surface gravity as a result of linear Stark broadening, while those of the higher Balmer lines (Hδ and higher) decrease with increasing $\log g$ due to the quenching of the atomic levels of the hydrogen atom. The quenching effect completely dominates the shape of the line profiles of Hϵ and higher Balmer lines. The simultaneous use of many Balmer lines thus provides a powerful tool to measure the surface gravity of hot white dwarfs, and it is arguably the most accurate technique to evaluate the mass distribution of a large sample of DA stars.

3.2. *Fitting Technique*

The technique used to derive the atmospheric parameters is similar to that used by Bergeron et al. (1990) and Daou et al. (1990) (see also Saffer et al. 1992a for a similar application to subdwarf B stars) where all the line profiles are fitted simultaneously. The first step is to normalize the line flux, in both observed and model spectra, to a continuum set to unity at a fixed distance from the line center. The comparison with model spectra, which are convolved with a Gaussian instrumental profile, is then carried out in terms of these line shapes only. This technique differs decisively from that of McMahan (1989) in that detailed line profiles are used and not the continuum spectrophotometry. The fitting technique employed here relies on the nonlinear least-squares method of Levenberg-Marquardt (Press et al. 1986), which is based on a steepest descent method. Here, the calculation of χ^2 is carried out using the normalized line profiles as defined above. The analysis is first performed assuming a constant arbitrary value of the standard deviation $\sigma = 1$ for each data point. With the values of $T_{\rm eff}$ and $\log g$ obtained by minimizing χ^2, a new value of σ is calculated from the rms deviation of the observed spectrum from the best-fit model spectrum. This is then propagated into the covariance matrix, from which the formal uncertainties of the fitted atmospheric parameters are obtained (Press et al. 1986). Although this approach forces the value of χ^2 to be near unity, it permits a form of internal error analysis when the uncertainty of each data point is not known in advance, as discussed by Press et al. (1986).

3.3. *Results and Error Estimation*

The $T_{\rm eff}$ and $\log g$ determinations for all program objects are reported in Table 1. The determination of individual stellar mass is discussed in the next section. Since the spectroscopic sample is homogeneous, the internal errors are of the same order, typically 100–300 K in $T_{\rm eff}$ and 0.02–0.06 in $\log g$. The *absolute* error of $T_{\rm eff}$ is about constant with effective temperature, and therefore the relative error, $\Delta T_{\rm eff}/T_{\rm eff}$, is larger for cooler stars. The quoted values are 1 σ errors provided by the fitting technique procedure and reflect basically the accuracy of the models to fit the data. One external error check can be obtained from multiple measurements of the same star. Independent observations of a subsample of 13 objects were therefore obtained on different nights. The results are given in Table

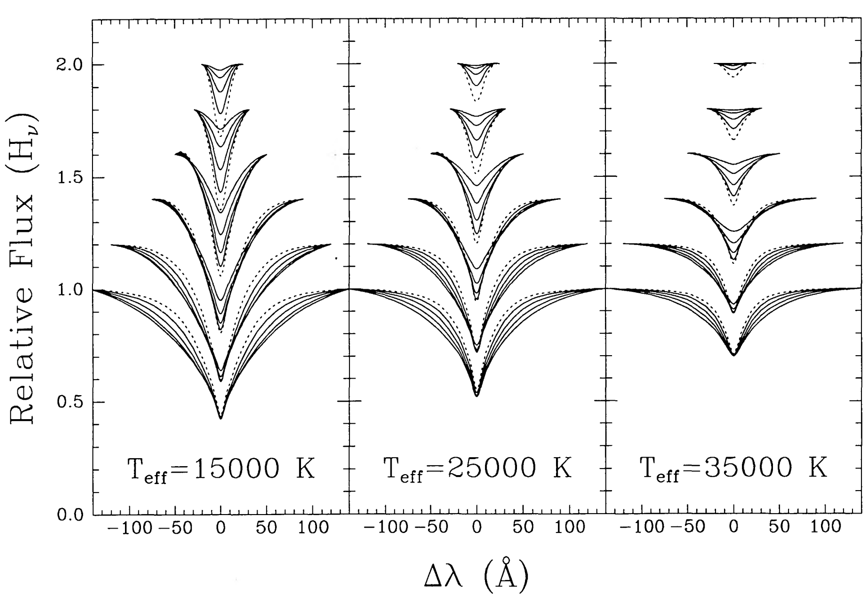

FIG. 3.—Theoretical line profiles of models at different effective temperatures and surface gravities. The models illustrated have $\log g = 7.0$ (0.5) 9.0; the dashed profiles are for the models at $\log g = 7.0$. The lines are (*bottom to top*) Hβ to H9 and have been normalized and offset vertically from each other.

TABLE 2

RESULTS OF MULTIPLE OBSERVATIONS

Name	$T_{\mathrm{eff}\,1}$	$\log g_1$	$T_{\mathrm{eff}\,2}$	$\log g_2$
G269-93	12970	8.00	13730	7.86
GD 421	30710	7.63	30520	7.66
PG 0216+144	27680	7.80	27520	7.85
Feige 22	19070	7.78	18990	7.80
G174-5	17050	8.26	16950	8.27
GD 41	35830	7.79	35530	7.87
GD 45	14880	7.61	15650	7.63
HZ 2	20790	7.94	21170	7.88
40 Eri B	16400	7.85	16730	7.88
GH 7-191	18960	8.00	19520	7.98
GH 7-233	23800	8.06	24440	8.03
HZ 7	21150	8.05	21840	8.03
HZ 14	27230	8.05	27430	8.11
GD 64	14260	7.71	14000	7.78
GD 64	14260	7.71	14040	7.79
G87-7	21060	8.10	21590	8.04
PG 1145+188	27240	7.77	26980	7.76
G261-45	16940	7.84	16820	7.95
G171-2	15900	7.91	16410	7.97

NOTE.—$\langle \Delta T_{\mathrm{eff}} \rangle = 350$ K, $\langle \Delta \log g \rangle = 0.049$.

2. The first two columns repeat the results given in Table 1, while the last two columns give the atmospheric parameters obtained from the independent observations. One object, GD 64, has been observed three times.

From Table 2, the mean error of the atmospheric parameters are $\langle \Delta T_{\mathrm{eff}} \rangle = 350$ K, and $\langle \Delta \log g \rangle = 0.049$ (or $\langle \Delta M/M_\odot \rangle \sim 0.03$), which are comparable to the internal errors. These individual errors are remarkably small and illustrate nicely the superior precision of the spectroscopic technique for determining atmospheric parameters of individual stars.

Several illustrative examples of the fitting technique are displayed in Figure 4. Objects of particular interests are shown, namely, the Hyades and the Pleiades (LB 1497) white dwarfs, the stars with gravitational redshift measurements (see Table 1), the most massive (GD 50) and least massive (PG 1101+364) objects in the sample. Finally, stars covering the whole range of atmospheric parameters are displayed as well. White dwarfs with unusually high surface gravity and mass show steep Balmer decrements (i.e., relatively weak high Balmer lines), while low-mass stars have high Balmer lines sharper and stronger than those in other stars of similar effective temperature.

3.4. *Determination of Stellar Masses*

For given values of T_{eff} and $\log g$, the stellar mass can be estimated from a mass-radius relation. In all previous analyses where masses were determined from surface gravity measurements, $M(g)$, the mass-radius relation employed was derived from the zero-temperature models of Hamada & Salpeter (1961) for a carbon-core composition. Zero-temperature relations are well justified for cool or high-mass white dwarfs. But as shown below, finite-temperature effects are important for this sample for which all stars are hotter than $T_{\mathrm{eff}} \sim 12{,}000$ K, including several objects with very low surface gravities. The masses were therefore estimated from the evolutionary models of Wood (1990) with pure carbon-core composition, surrounded by a helium layer of mass $\log q(\mathrm{He}) \equiv \log(M_{\mathrm{He}}/M_*) = -4$, which span the relevant mass range of 0.4–1.2 $M_\odot$ (for more massive objects, the masses were derived from the Hamada-Salpeter relation). Additional carbon sequences at 0.2 and 0.3 $M_\odot$ have been kindly provided by M. A. Wood for the purpose of this analysis. The complete results are reported in Table 1. The absolute magnitudes, M_V, have been calculated following the prescription of Wesemael et al. (1980).

The importance of finite-temperature effects for determining the stellar masses of the sample can be appreciated by comparing the masses obtained from the models of Wood (1990) with those obtained from the zero-temperature models of Hamada-Salpeter discussed above. As shown in Figure 5, individual masses can be underestimated by large amounts if zero-temperature models are used instead of realistic cooling sequences. The difference can be as large as 0.08 $M_\odot$ in a few cases. Even at $\sim 14{,}000$ K, the average difference is of the order of 0.02 $M_\odot$.

Experiments with several other model sequences of Wood (1990) allow us to estimate the effects of assuming different core/envelope compositions on the derived masses. If all program stars are fitted with models having 0.5/0.5 mixed carbon-oxygen cores and $\log q(\mathrm{He}) = -4$, the individual masses of Table 1 would decrease by at most 0.004 $M_\odot$. The thickness of the helium layer is also a small effect. In the $\log q(\mathrm{He}) = -2$, $M = 0.6\ M_\odot$ models, the radius is about 0.7% larger at $T_{\mathrm{eff}} = 25{,}000$ K, or equivalently, the mass determined for such a star would be underestimated by only $\sim 0.004\ M_\odot$. The effect of adding a thin hydrogen layer of mass $\log q(\mathrm{H}) = -10$ on top of the $\log q(\mathrm{He}) = -4$ helium layer is completely negligible. If the hydrogen layer is thick, however, the effect could be large: For a 0.6 $M_\odot$ model with $\log q(\mathrm{H}) = -4$, the radius is 7% larger at $T_{\mathrm{eff}} = 25{,}000$ K, and the mass of such a star would be underestimated by $\sim 0.04\ M_\odot$. However, there is now growing evidence that the hydrogen layer of DA white dwarfs is indeed very thin (see, e.g., Fontaine & Wesemael 1987).

3.5. *Comparison with Previous Atmospheric Parameter Determinations*

The atmospheric parameters can now be compared to previous estimates. In Figure 6, the effective temperatures and surface gravities are compared to those obtained by KSW, WK, and McMahan (1989). Since the analysis of WK is concentrated in a region where the sensitivity of a Balmer jump to surface gravity is the largest ($8000 \lesssim T_{\mathrm{eff}} \lesssim 16{,}000$ K), there is little overlap with the spectroscopic sample of Table 1. The agreement with the effective temperatures obtained by KSW is good, although their values are systematically hotter than the spectroscopic temperatures by ~ 300 K. Such an offset is not seen in the comparison with WK, although the number of stars in common with their analysis is small. There are some discrepant results with the analysis of KSW for a few isolated cases: LB 1497 ($T_{\mathrm{eff}} = 28{,}574$ K) and GD 125 ($T_{\mathrm{eff}} = 17{,}354$ K). For the latter object, KSW obtained a large value of χ^2 for their fit. For LB 1497, the temperature obtained in this analysis, $T_{\mathrm{eff}} = 32{,}920$ K, is in excellent agreement with a recent determination by Wegner, Reid, & McMahan (1991) who obtained $T_{\mathrm{eff}} = 32{,}000 \pm 1000$ K.

The agreement with the results of McMahan (1989) is poor, in particular for the hottest objects. Considering the discussion above, this seems at odds with the analysis of McMahan (1989) who concluded that there appears to be no systematic disagreement between his temperature determinations and those

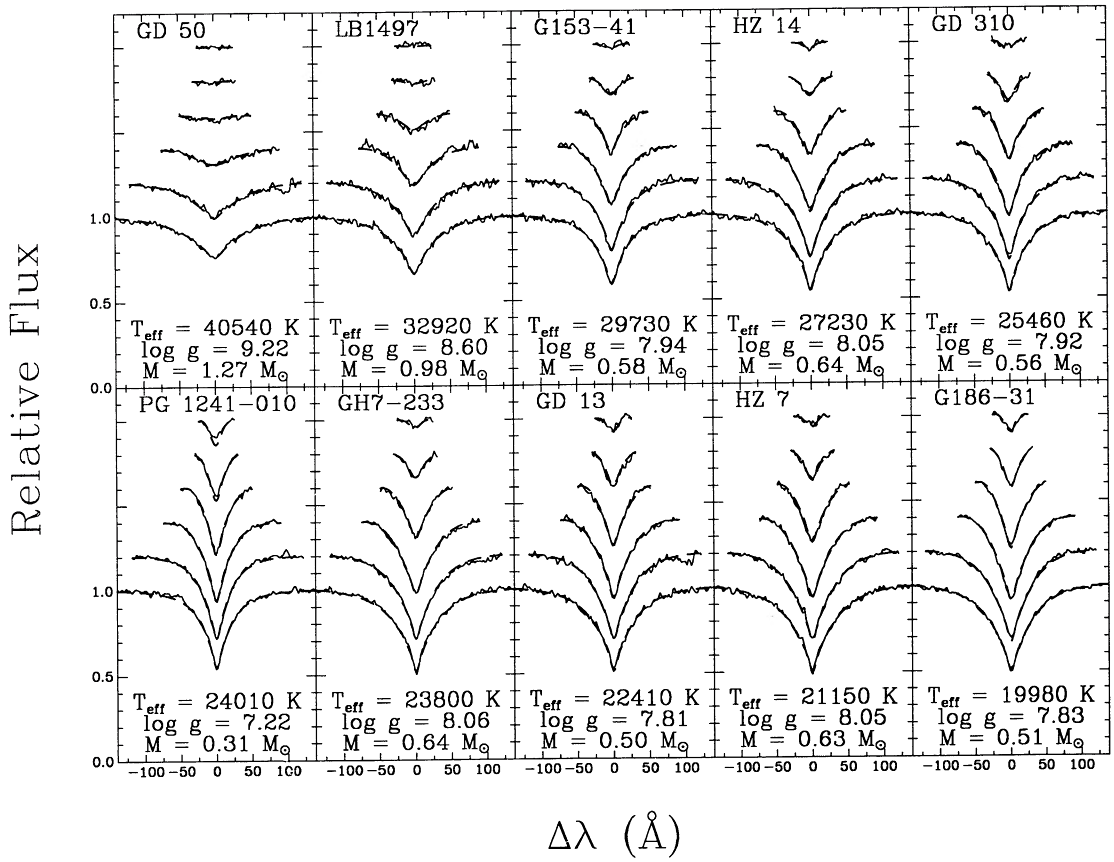

FIG. 4*a*

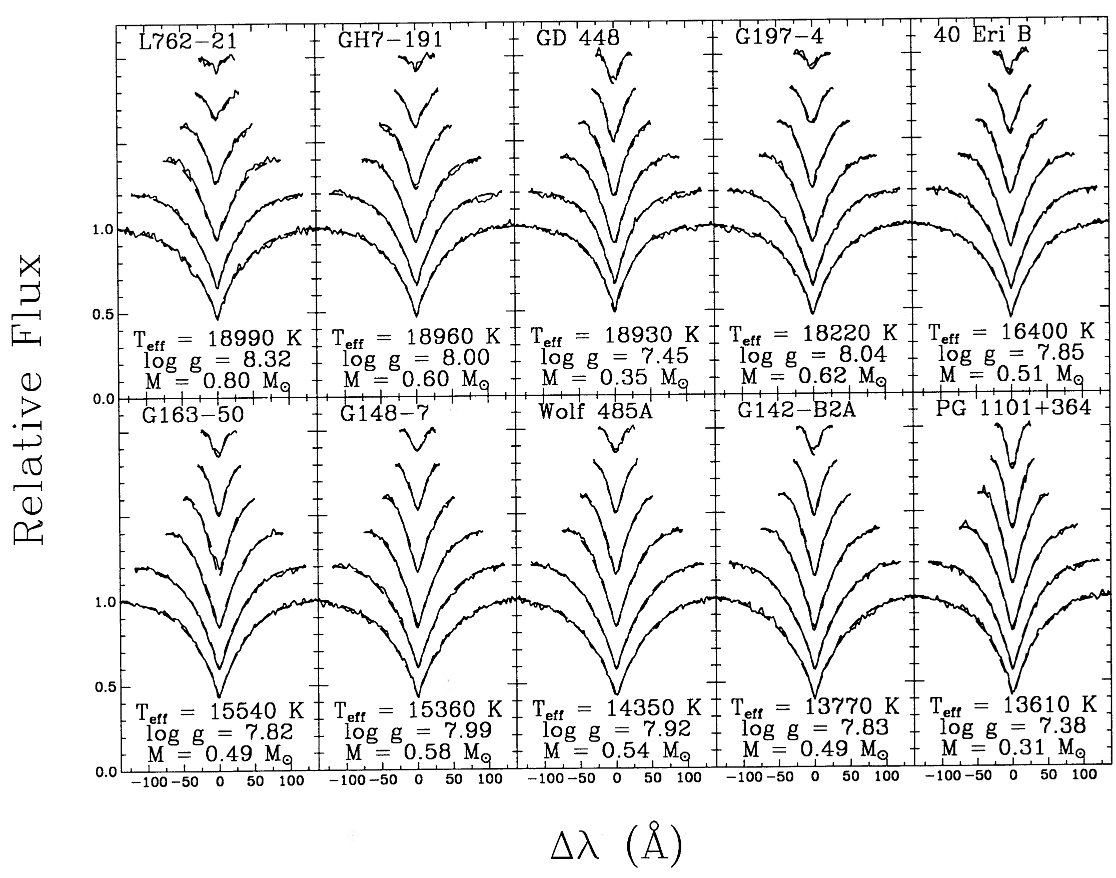

FIG. 4*b*

FIG. 4.—Fits to the individual Balmer lines for a repesentative subsample of program objects. The lines range from Hβ (*bottom*) to H9 (*top*), each offset vertically by a factor of 0.2.

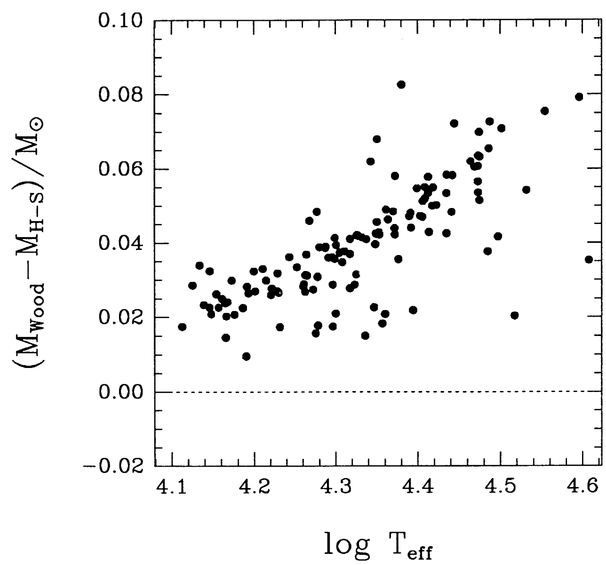

FIG. 5.—Differences between stellar masses estimated from the evolutionary models of Wood (1990) and the zero-temperature models of Hamada-Salpeter as a function of effective temperature. All models are for carbon-core ompositions.

of KSW. However, examination of his Figure 1 indicates that there is a systematic shift of ~1300 K for stars hotter than $T_{eff} = 15{,}000$ K. All these stars in common with both KSW and McMahan (1989) have been reobserved here in spectroscopy and the same systematic shift is observed. If *all* stars in common with McMahan (1989) are considered, the offset is then more than 1500 K. The differences are even larger above $T_{eff} = 30{,}000$ K. It is especially at high temperatures that his technique of fitting the energy distribution of low-resolution optical spectra is likely to fail because of the lack of sensitivity of the Paschen continuum to variations of effective temperature (see, in particular the case of GD 50 discussed by Bergeron et al. 1991a).

The comparison with previous surface gravity determinations is also displayed in Figure 6. The values of log g as determined by KSW are systematically lower than our spectroscopic determinations, and also exhibit a much larger dispersion. This is probably due to the lack of sensitivity to log g variations of color indices for stars at high effective temperatures. Again, although the number of stars in common with the analysis of WK is small, that systematic trend is not seen in the comparison. The results of McMahan (1989) are in good agreement with the values determined here, with the largest differences again occurring for the hottest objects (see above).

4. COMPARISON WITH VARIOUS TECHNIQUES

In previous sections, the spectroscopic technique has been shown to provide very accurate individual determination of atmospheric parameters. The errors of each measurement are small enough that the *relative* values of log g are probably reliable. But the technique is also new and relies strongly on the accuracy and validity of the Hummer-Mihalas formalism used in the model calculations. Therefore, the *absolute* values of log g may suffer from what is like a zero-point offset, and it is important to compare the individual measurements with results obtained from independent techniques. Here, the spectroscopic masses are compared to masses inferred from radius measurements using published trigonometric parallax, and masses determined from gravitational redshift measurements, for stars in common with this sample.

4.1. *Trigonometric Parallax Techniques*

Table 3 lists the objects for which trigonometric parallax measurements are available. All listed values are from van Altena, Lee, & Hoffleit (1992). From these values, and the V magnitudes given in Table 1, one can obtain the absolute magnitude, M_V. Then, by first assuming a value of log $g = 8.0$, and the T_{eff} value from Table 1, the bolometric correction is calculated and used to derive the luminosity and radius of the star. The radius is then converted into mass via the evolutionary models of Wood (1990), and a new value of log g is derived. The whole procedure is then iterated until a self-consistent solution for log $g(\pi)$ is achieved. The uncertainty in the value of log g is calculated simply here by averaging the log g differences at $\pi \pm \sigma_\pi$ (or $\pi + \sigma_\pi$ for stars with $\sigma_\pi > \pi$). The results of the analysis are reported in Table 3 (with the uncertainties in parentheses) and in Figure 7.

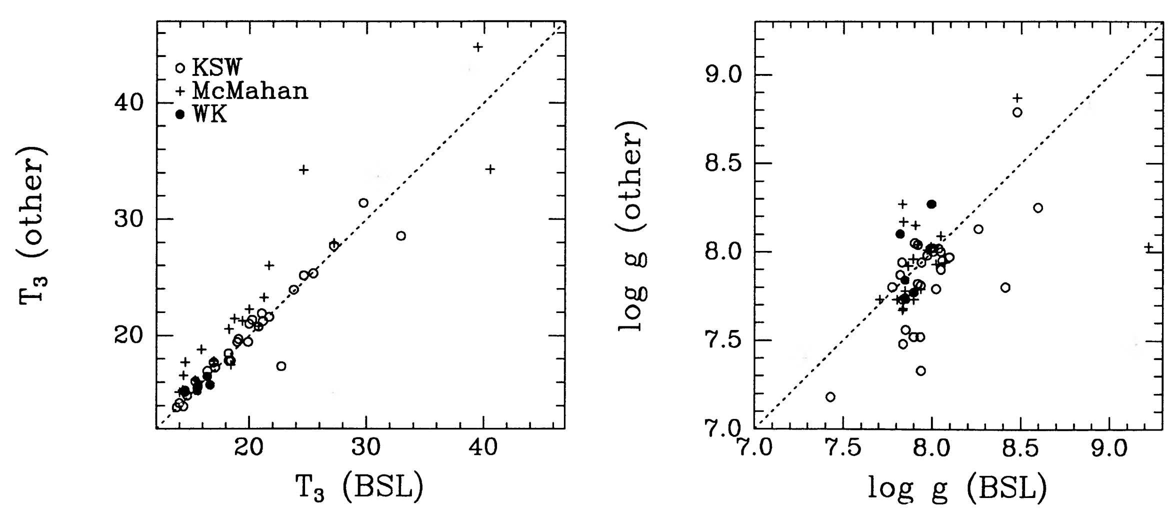

FIG. 6.—Comparison of T_{eff} and log g determinations given in Table 1 with values obtained by KSW, WK, and McMahan (1989). The effective temperatures are in units of 10^3 K. The dashed line is the 1:1 correspondence.

TABLE 3

RESULTS FOR THE PARALLAX ENSEMBLE

Name	$\pi(\sigma_\pi)$	$R/R_\odot$	log $g(\pi)$	log g(BSL)
G153-41	0.0086 (0.0153)	0.0327	6.81 (1.348)	7.94
PG 0817+386	0.0252 (0.0025)	0.0039	9.30 (0.056)	8.00
G104-27	0.0282 (0.0021)	0.0118	8.12 (0.102)	7.94
GD 222	0.0294 (0.0024)	0.0117	8.13 (0.113)	7.84
H Per 1166	0.0148 (0.0045)	0.0226	7.19 (0.373)	7.83
G87-7	0.0626 (0.0018)	0.0111	8.21 (0.040)	8.10
HZ 2	0.0079 (0.0083)	0.0399	6.38 (1.029)	7.94
G238-44	0.0307 (0.0041)	0.0169	7.58 (0.193)	7.90
G186-31	0.0704 (0.0021)	0.0133	7.94 (0.045)	7.83
L711-10	0.0425 (0.0031)	0.0152	7.74 (0.110)	7.93
G142-50	0.0244 (0.0027)	0.0126	8.03 (0.154)	7.80
GH 7-91	0.0177 (0.0050)	0.0154	7.71 (0.383)	8.00
GD 163	0.0253 (0.0028)	0.0127	8.00 (0.156)	7.97
G93-48	0.0404 (0.0025)	0.0140	7.86 (0.094)	8.02
G197-4	0.0227 (0.0044)	0.0155	7.70 (0.277)	8.04
G261-45	0.0387 (0.0044)	0.0138	7.88 (0.168)	7.84
40 Eri B	0.2065 (0.0021)	0.0133	7.94 (0.016)	7.85
G171-2	0.0293 (0.0069)	0.0132	7.94 (0.317)	7.91
G240-51	0.0363 (0.0041)	0.0140	7.86 (0.168)	7.90
G163−50	0.0206 (0.0087)	0.0294	6.81 (0.462)	7.82
G148-7	0.0315 (0.0023)	0.0137	7.89 (0.111)	7.99
GD 178	0.0208 (0.0048)	0.0175	7.50 (0.333)	8.00
G231-40	0.0516 (0.0062)	0.0161	7.62 (0.184)	7.85
Wolf 485A	0.0611 (0.0028)	0.0139	7.86 (0.071)	7.92
GD 64	0.0232 (0.0030)	0.0168	7.55 (0.197)	7.71

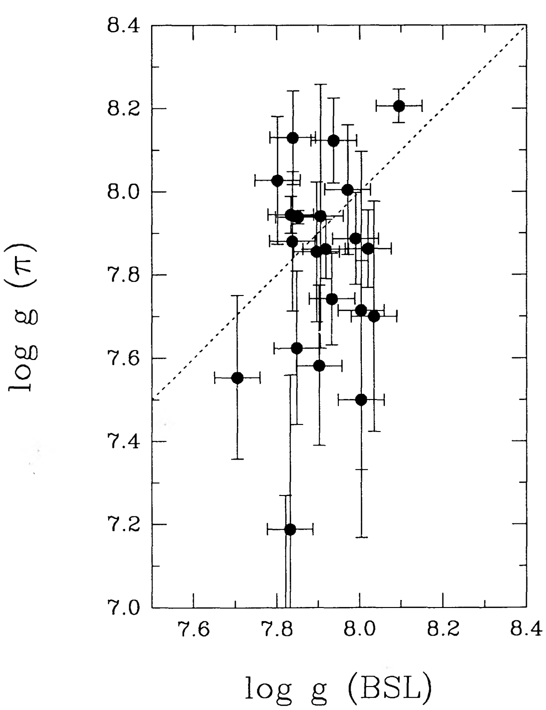

FIG. 7.—Comparison of surface gravities obtained from parallax measurements with those obtained from spectroscopy. The size of the error bars of the spectroscopic measurements corresponds to the external error discussed in § 3.3. Note that both axes are on the same scale. The dashed line is the 1:1 correspondence.

As mentioned in § 1.1, masses estimated from stellar radii, $M(R)$, might be *systematically* different than the values derived from gravities via stellar atmospheres analyses, $M(g)$. Such an effect is not observed here: If only the stars with $\Delta(\log g) < 0.5$ are considered in Table 3, the average values are log $g(\pi) = 7.842$, $\sigma = 0.445$, and log $g(\text{BSL}) = 7.913$, $\sigma = 0.093$. At the least, this suggests that, on average, the spectroscopic determinations are consistent with the solutions obtained from trigonometric parallaxes. The individual determinations, however, differ significantly in many cases, well beyond the quoted uncertainties. The larger dispersion of the log g determinations obtained from trigonometric parallaxes suggest that the errors of the trigonometric parallax measurements are likely to be underestimated.

4.2. *Gravitational Redshift Measurements*

White dwarf masses can also be estimated from the direct measurement of the gravitational redshift velocity, $v_{\text{GR}} = GM/cR$. This last relation indicates that the mass can be inferred only through a suitable mass-radius relationship. All previous analyses have used the Hamada-Salpeter models with carbon configurations. Because of the finite-temperature effects discussed above, however, the masses have been redetermined from the published values of the velocities using the same evolutionary sequence of Wood (1990) discussed in § 3.4. The uncertainty of the mass determination has been derived from the error of the velocity measurement only. The results of the comparison are summarized in Table 4 and displayed in Figure 8. Multiple measurements of the same object from different investigations were considered independently. These independent values agree within the given uncertainties except for G142-B2A. For this star, Wegner & Reid (1991) obtained a result which is significantly different from their own previous estimate.

The average mass obtained from gravitational redshift determinations is $M = 0.629\ M_\odot$ with a dispersion of $\sigma = 0.144\ M_\odot$, in agreement with the average mass derived from spectroscopy, $M = 0.611\ M_\odot$, with a somewhat smaller dispersion of $\sigma = 0.129\ M_\odot$. If the new measurement of G142-B2A is

TABLE 4

COMPARISON WITH GRAVITATIONAL REDSHIFT MEASUREMENTS

Name	v_{GR} (km s^{-1})	$M_{\text{GR}}/M_\odot$	$M_{\text{BSL}}/M_\odot$	References
HZ 14	21.8 (6.4)	0.510 (0.086)	0.639 (0.032)	1
	29.7 (5.8)	0.608 (0.067)	0.639 (0.032)	2
GH 7-233	30.9 (2.5)	0.616 (0.028)	0.637 (0.032)	1
	35.7 (3.8)	0.669 (0.040)	0.637 (0.032)	2
HZ 7	35.6 (7.3)	0.665 (0.077)	0.628 (0.032)	1
GH 7-191	36.1 (3.4)	0.668 (0.036)	0.599 (0.031)	1
LB 1497	84.0 (9.0)	1.025 (0.043)	0.983 (0.033)	3
40 Eri B	23.9 (3.0)	0.520 (0.040)	0.510 (0.028)	4
	26.5 (1.5)	0.554 (0.019)	0.510 (0.028)	5
G163-50	20.1 (3.2)	0.466 (0.046)	0.492 (0.028)	6
	19.7 (3.0)	0.460 (0.043)	0.492 (0.028)	4
G148-7	27.0 (3.0)	0.558 (0.038)	0.583 (0.032)	4
Wolf 485A	24.9 (3.2)	0.530 (0.042)	0.540 (0.030)	6
	24.9 (3.0)	0.530 (0.039)	0.540 (0.030)	4
L762-21	51.2 (12.0)	0.808 (0.099)	0.796 (0.036)	6
	55.0 (9.0)	0.839 (0.070)	0.796 (0.036)	2
G142-B2A	27.4 (3.0)	0.561 (0.038)	0.492 (0.028)	4
	44.0 (4.0)	0.740 (0.037)	0.492 (0.028)	2

REFERENCES.—(1) Wegner, Reid, & McMahan 1989; (2) Wegner & Reid 1991; (3) Wegner, Reid, & McMahan 1991; (4) Wegner & Reid 1987; (5) Koester & Weidemann 1991; (6) Koester 1987.

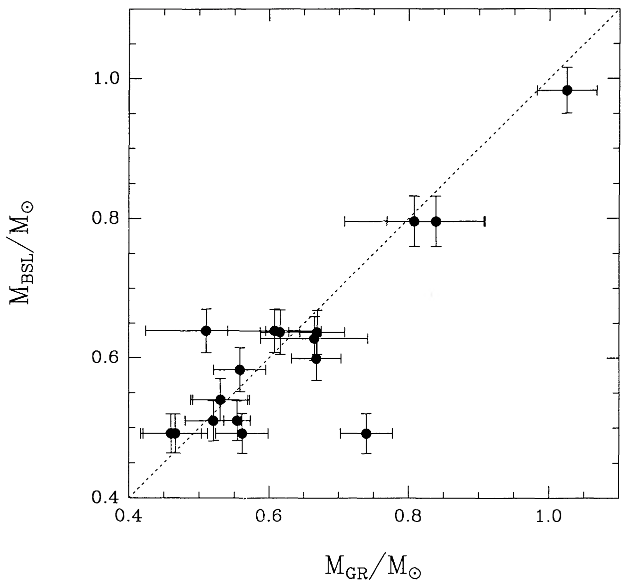

FIG. 8.—Comparison of stellar masses derived from gravitational redshift measurements with those obtained from spectroscopy. The dashed line is the 1:1 correspondence.

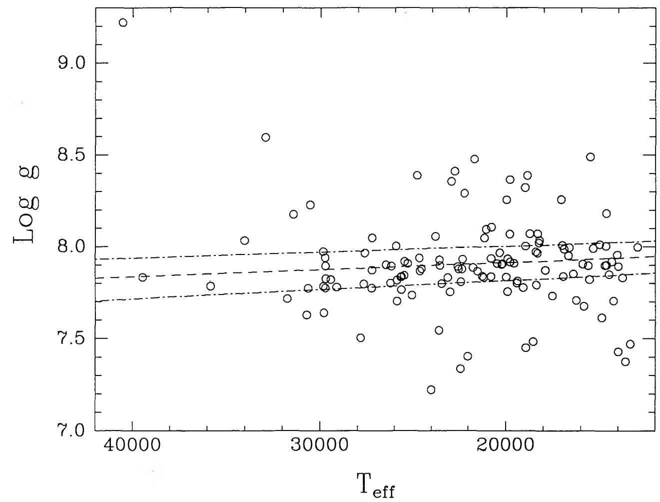

FIG. 10.—Distribution of surface gravity with effective temperature for all objects. The dashed line indicates the locus of the 0.55 $M_\odot$ evolutionary models of Wood (1990), and the lower and upper dash-dotted lines correspond to the 0.5 and 0.6 $M_\odot$ models, respectively.

excluded from the analysis, the mean masses then agree to within $\sim 0.005\ M_\odot$.

5. THE MASS DISTRIBUTION OF DA STARS

5.1. *Results*

The surface gravity and mass distributions of all DA stars in the spectroscopic sample are presented in Figure 9. The surface gravity distribution has a mean value of $\log g = 7.909$ with a standard deviation of $\sigma(\log g) = 0.257$, while the mass distribution has a mean value of $M = 0.562\ M_\odot$ with a standard deviation of $\sigma(M) = 0.137\ M_\odot$. Because of finite-temperature effects, the mean surface gravity is not constant over the range of effective temperature considered here, and therefore, is not a very meaningful quantity in the present context. As an example, a 0.55 $M_\odot$ white dwarf will have a surface gravity of $\log g = 7.83$ at $T_{eff} = 42{,}000$ K and $\log g = 7.95$ at $T_{eff} = 12{,}000$ K. This is better illustrated in Figure 10, where the distribution of surface gravity with effective temperature for all objects is shown. Most objects lie close to the evolutionary model at 0.55 $M_\odot$ with a very small dispersion. There is also no

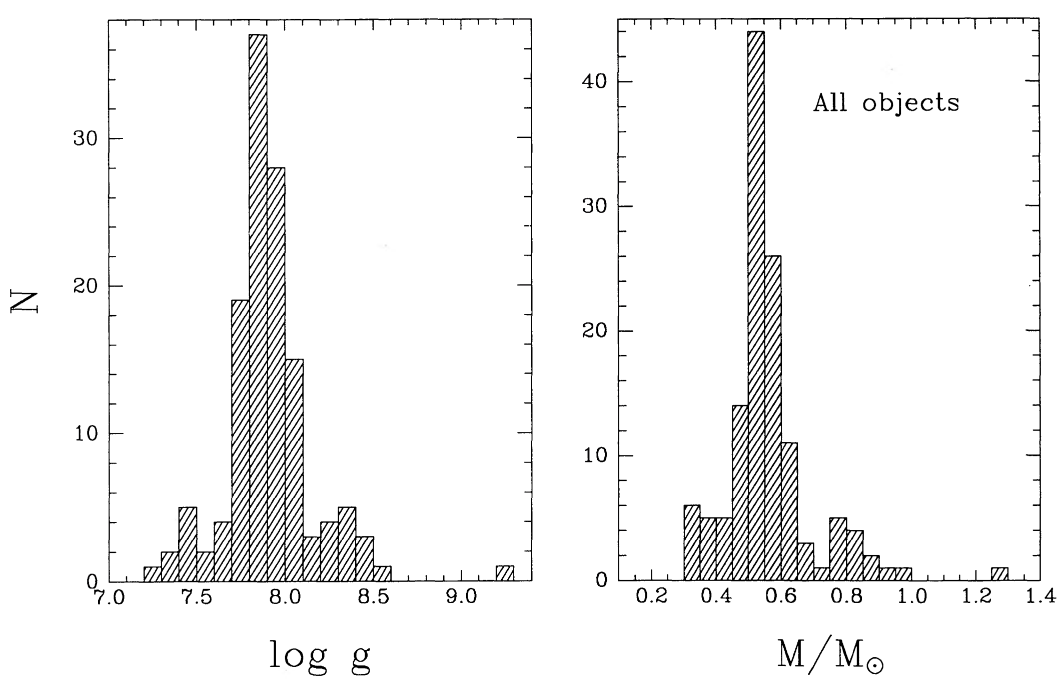

FIG. 9.—Surface gravity and mass distributions for all 129 objects in the spectroscopic sample. The surface gravity distribution has a mean value of $\log g = 7.909$ with a standard deviation of $\sigma(\log g) = 0.257$, and the mass distribution has a mean value of $M = 0.562\ M_\odot$ with a standard deviation of $\sigma(M) = 0.137\ M_\odot$.

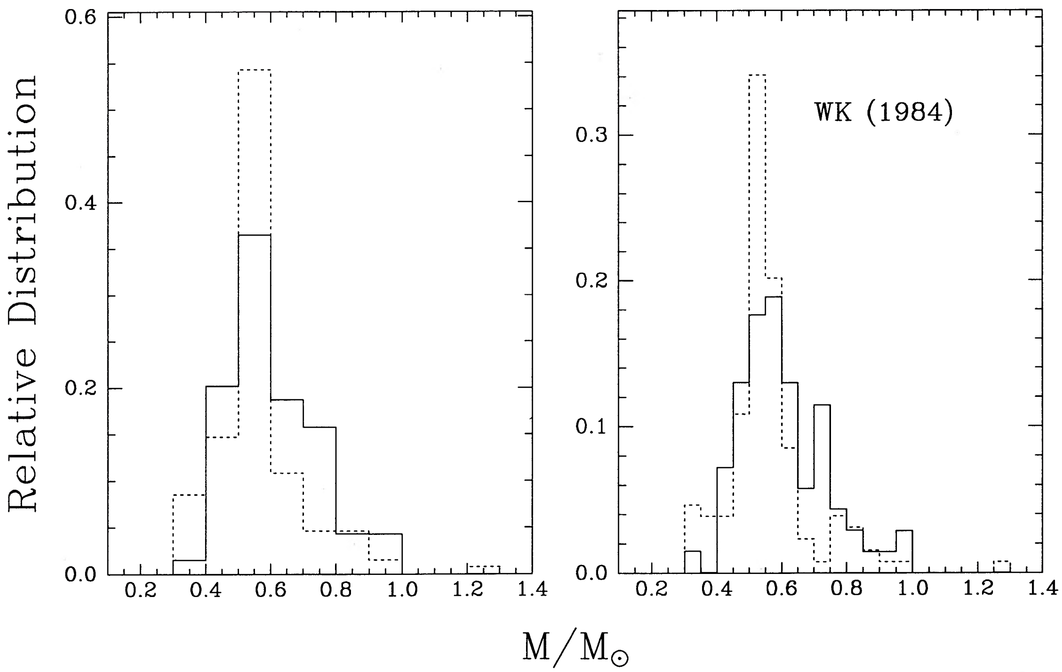

FIG. 11.—Comparison of the *relative* mass distribution derived from spectroscopy (*dashed line*) with that obtained by WK (*solid line*), using different mass resolutions. The mean mass of WK is $M = 0.603\ M_\odot$ with a dispersion of $\sigma(M) = 0.133\ M_\odot$.

obvious correlation of log g with $T_{\rm eff}$ that could not be accounted for by evolutionary considerations alone (Wood & Bergeron 1992).

In order to compare the mass distribution obtained from spectroscopy with those of WK and McMahan (1989), the original $T_{\rm eff}$ and log g values given in these analyses have been used along with the evolutionary models of Wood (1990) to derive stellar masses consistent with the present analysis. The results have been converted into relative mass distributions with mass resolutions of 0.05 and 0.10 $M_\odot$. The comparisons are displayed in Figures 11 and 12. The mean masses and standard deviations are $M = 0.603$, $\sigma(M) = 0.133\ M_\odot$ and $M = 0.571$, $\sigma(M) = 0.188\ M_\odot$ for the sample of WK and McMahan (1989), respectively. These mean values are slightly larger by $\sim 0.025\ M_\odot$ than the original values given in § 1.2, which reflect the importance of finite-temperature effects in determining stellar masses. The mean mass derived from spectroscopy is lower than these two determinations, but with a

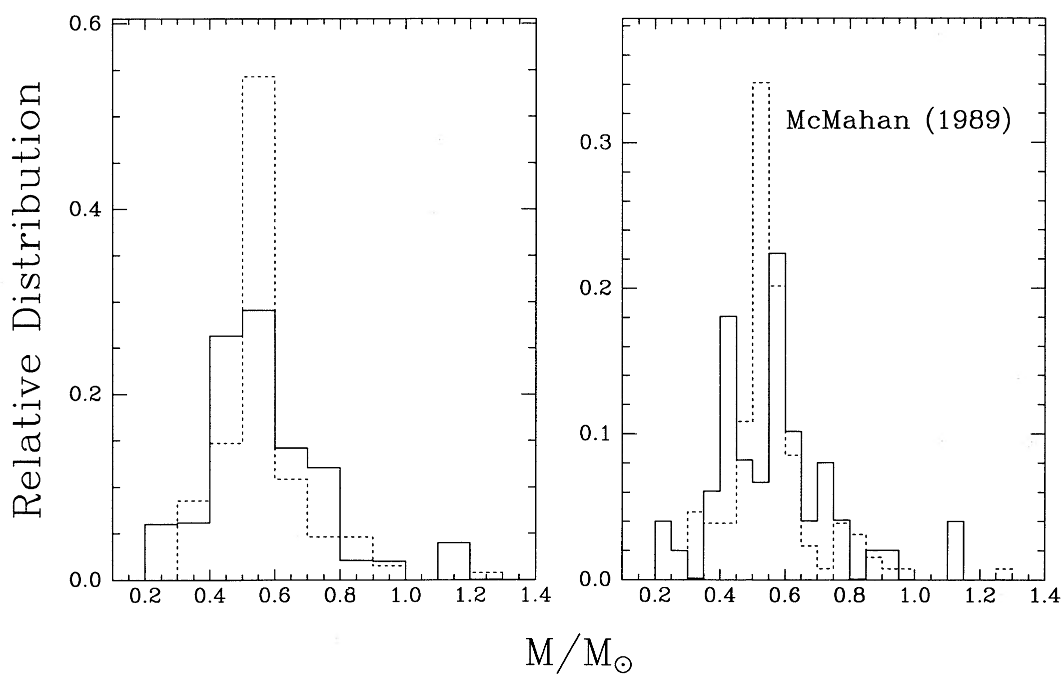

FIG. 12.—Same as Fig. 11 but with the results of McMahan (1989). The mean mass of McMahan (1989) is $M = 0.571\ M_\odot$ with a dispersion of $\sigma(M) = 0.188\ M_\odot$.

standard deviation comparable to that of WK. When displayed on a 0.10 $M_\odot$ mass resolution scale, all distributions exhibit a sharp and well-defined peak around 0.55 $M_\odot$ after a steep increase at 0.40–0.45 $M_\odot$, and a flatter tail toward higher masses. This skew of the observed mass distribution is expected from stellar and Galactic evolution if white dwarfs evolve from an initial mass function heavily weighted toward lower initial masses (Koester & Weidemann 1980; Yuan 1989).

The precision of the spectroscopic technique allows one to look at the mass distribution at a higher mass resolution of 0.05 $M_\odot$. These results are displayed in Figures 11 and 12 as well. At this resolution, the mass distributions of WK and McMahan (1989) flatten, and the central peak gets substantially broader. The McMahan distribution even shows a minimum in the 0.45–0.55 $M_\odot$ range. The central peak of the mass distribution derived from spectroscopy, however, remains very well defined. In contrast to previous investigations, the mass distribution now looks remarkably symmetric, with a narrower central peak and flatter tails which contain clear cases of low- and high-mass objects. The mean mass is comparable to, or somewhat lower than, values reached in previous analyses. Perhaps a more interesting quantity is the *mode* of the mass distribution which falls in the range 0.50–0.55 $M_\odot$ where more than 30% of the stars are found. The dispersion is therefore even smaller than previously asserted by KSW and WK: the value of 0.10 $M_\odot$ quoted by KSW is defined as the semi-interval which contains two-thirds of their sample. If this definition is adopted here, about 75% of the stars in the sample are contained within an interval of $\pm 0.10\ M_\odot$ (or $\frac{2}{3}$ of the stars are contained within an interval of $\pm 0.075\ M_\odot$). This very narrow distribution is also reflected in Figure 10. The median of the distribution is also a quantity of interest and has a value of $M = 0.540\ M_\odot$.

The details seen in the mass distribution are the result of both the size of this sample and the improved sensitivity of the spectroscopic technique over previous methods to resolve with high accuracy the fine structure present in the mass distribution of DA white dwarfs. The results presented here indicate that the *typical* mass of a DA white dwarf is significantly lower than the canonical value of 0.6 $M_\odot$ used in most studies. Had the Hamada-Salpeter mass-radius relation been used instead, the mode would have been shifted to an even lower mass range of 0.45–0.50 $M_\odot$. Note that this last result is consistent with the conclusions reached by KSW when their $M(g)$ analysis is restricted to stars with $T_{\rm eff} > 13{,}000$ K.

5.2. *Selection Effects*

Since the *observed* mass distribution derived here is drawn from a magnitude-limited sample of DA stars, selection effects operate against larger mass (smaller radius) stars, and therefore the *true* distribution could potentially be shifted to higher masses. For example, Shipman (1979) corrected his value for the mean mass from 0.55 to 0.75 $M_\odot$. Koester (1984) has shown, however, that this correction factor depends on the dispersion of the observed mass distribution, and therefore on the accuracy of the technique used in the analysis. He noted that the dispersions of the samples of KSW and WK are smaller than that of Shipman (1979). Hence, the correction factor for their sample is only of the order of 0.03 $M_\odot$.

Alternatively, when the mass distribution is obtained from a magnitude-limited sample, the correction can be calculated explicitly. This has been done, for example, by McMahan (1989) who obtained corrected average values by dividing each mass bin by the volume sampled in that bin which is proportional to the cube of the corresponding stellar radius (see Koester 1984 for more details). The same technique applied here to the spectroscopic sample yields a corrected mean mass of 0.712 $M_\odot$. It is found, however, that this result is very sensitive to the presence of outliers in the mass distribution. As an example, the corrected mean mass drops to 0.621 $M_\odot$ if GD 50, the most massive star in the sample, is excluded. The value is further reduced to 0.609 $M_\odot$ if LB1497, the Pleiades white dwarf purposely added to the sample, is excluded as well. It is therefore reasonable to ask if these mass bins which contain a very small number of stars are representative of the true distribution. If the analysis is restricted to mass bins in the range $0.35 < M/M_\odot < 0.70$, which defines the Gaussian distribution of the central peak, the mean mass increases from 0.535 $M_\odot$ to a corrected value of only 0.547 $M_\odot$.

The observed sample might be also biased toward stars with high proper motions since all the objects were selected from the McCook & Sion (1987) catalog, most of which were discovered in proper motion surveys. A more appropriate ensemble is provided by color-selected samples such as the one defined in the Palomar Green survey. The mass distribution of the PG subgroup is displayed in Figure 13. The mean mass is $M = 0.562\ M_\odot$ with a dispersion of $\sigma(M) = 0.126\ M_\odot$, in excellent agreement with the results obtained from the complete sample, which indicates that this selection effect is negligible. The correction to the mean mass is 0.063 $M_\odot$ (for an average value of $M = 0.625\ M_\odot$), and is therefore much smaller than that obtained from the complete sample, though somewhat larger than that of Koester (1984). However, Koester did not calculate the correction from the mass distribution itself, but instead derived it from the values of the mean mass and standard deviation obtained by KSW (see his Table 2). This approach is less sensitive to the presence of outliers in the mass distribution.

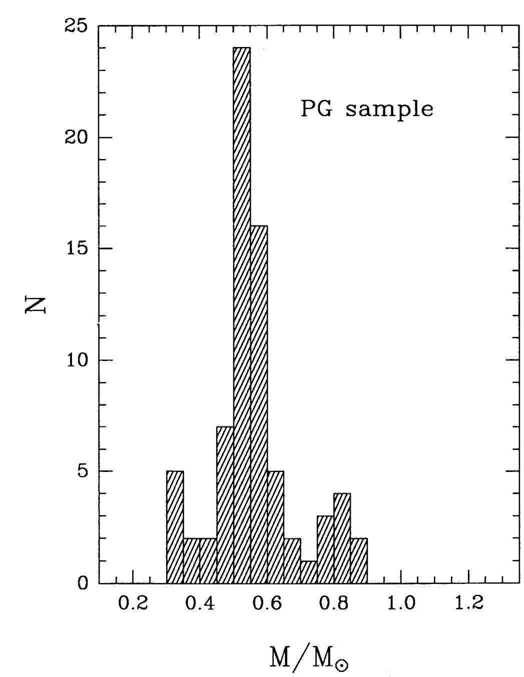

FIG. 13.—Mass distribution for the Palomar-Green objects. The mean mass is $M = 0.562\ M_\odot$ with a dispersion of $\sigma(M) = 0.126\ M_\odot$.

The details of the correction procedure are still uncertain, especially considering that many stars fainter than the limit $V = 15.5$ have been included in the sample (see Fig. 1), and it seems more appropriate to simply refer to the *observed* mass distribution of DA white dwarfs. Only by measuring the non-Gaussian high- (and/or low-) mass tail of the distribution accurately—with a very large sample—can the size of the correction to the mean mass be correctly assessed. However, the position of the peak of the distribution—or the median of the distribution—is affected little.

5.3. *Astrophysical Implications*

While these results confirm the assertion by KSW and WK of a sharply peaked mass distribution, the function obtained from spectroscopy has two features which do not seem consistent with the conclusions of WK. First, these authors wrote: "it will appear from this study that there remain actually no convincing cases for which $\log g < 7.75$ or $M < 0.42\ M_\odot$, and only very few with $\log g > 8.25$ or $M > 0.72\ M_\odot$." The mass distribution presented here appears to have what may be even a separate component of about 10 low-mass ($\leq 0.40\ M_\odot$) white dwarfs, in addition to a few objects near $0.8\ M_\odot$ and one discrepant case near $1.3\ M_\odot$. The low-mass stars span most of the $T_{\rm eff}$ range (see Fig. 10) and are obvious from inspection of their spectra, as they have much sharper Balmer lines generally including one more high series member than for spectra of objects having similar effective temperatures and normal surface gravities. This appearance is consistent with the lower atmospheric pressure found in DA stars with smaller surface gravity.

The apparent sequence of low-mass DA stars is of significance to stellar evolution theory which cannot accommodate objects evolving to white dwarfs with masses below the core-helium ignition limit (~ 0.45–$0.50\ M_\odot$) from single star evolution within the lifetime of this Galaxy. The result suggests that $\sim 10\%$ of DA white dwarfs could be products of close binary evolution as predicted by such authors as Tutukov & Yungelson (1987) and Iben & Tutukov (1987). These systems should include at least one visible helium-core degenerate whose core mass was truncated by case B mass transfer before helium ignition was reached. Binary periods may be determined by searches for radial velocity or line profile variations. One confirmed case and some promising candidates for close binary white dwarfs—which may have systematically lower than their average mass—are discussed in Bragaglia et al. (1990; see also Foss, Wade, & Green 1991). If double degenerate cores also emerge from common-envelope evolution with small enough separations to merge within the lifetime of the Galaxy, the resulting mergers could produce a single product with average or higher than average mass (Iben 1990). Thus, the white dwarf mass distribution could include close binary stars or products of close binary evolution. If the low-mass and some high-mass objects in the mass distribution are indeed the product of binary evolution, the remaining objects, presumably formed from single star evolution, will exhibit an even narrower distribution.

From evolutionary considerations, the mass of these low surface gravity objects should be estimated from evolutionary models with helium configurations. Inspection of the relevant figures in the Hamada & Salpeter (1961) mass-radius relations indicates that there are no significant differences between the carbon and helium configuration models at $M \sim 0.3\ M_\odot$. The finite-temperature effects cannot be measured directly because of the lack of extensive evolutionary models with helium cores published in the literature, although these effects are expected to be small.

The results presented here and the assessment of the previous work suggests that the peak or median mass of DA white dwarfs may be significantly lower than the value near $0.6\ M_\odot$ arrived at in the best previous studies. If true, this would have some consequences for earlier phases of stellar evolution. While $0.04\ M_\odot$ might seem at first glance to be a small difference, it implies that a significantly smaller fraction of white dwarfs could be expected to have passed through the planetary nebula phase. In particular, for masses below about $0.55\ M_\odot$ (more than 50% of the stars in the sample), the rate of post–asymptotic giant branch (AGB) stellar evolution should be too slow for an ejected nebula to be excited before it has dissipated (Weidemann & Koester 1983). For masses much below 0.55 $M_\odot$, the stars could not have passed through the luminous AGB or Mira phases, but rather would have had sufficiently higher rates of mass loss to truncate evolution on the "early" AGB or even the horizontal branch (see the next paragraph). Note that the uncertainty in the correction to the average mass discussed in § 5.2 will not affect substantially the fraction of white dwarfs observable as planetary nebulae.

White dwarfs with masses near $0.5\ M_\odot$ may have come directly from the subdwarf B and some subdwarf O stars, if such stars are core-helium–burning objects on the "extended" horizontal branch, as defined by Greenstein & Sargent (1974). It is known that these hot subdwarfs exist in large numbers (though correspondingly long lifetimes for helium burning may apply) and that those found at high Galactic latitudes belong predominantly to the disk population (Baschek & Norris 1975; Green et al. 1986; Saffer, Liebert, & Green 1992b).

6. OBJECTS OF PARTICULAR ASTROPHYSICAL INTEREST

6.1. *LB 1497*

Among the stars assigned a mass substantially higher than the peak value is LB 1497, the star likely to be the only evolved member of the Pleiades. In contrast to the low-mass stars, its spectrum shows very broad lines with a decrement clearly steeper than average. Assuming LB 1497 has the Pleiades radial velocity, Wegner, Reid, & McMahan (1991) obtained recently a gravitational redshift measurement of $v_{\rm GR} = +84 \pm 9$ km s^{-1}. This corresponds to a mass of $M = 1.025 \pm 0.043\ M_\odot$ using the evolutionary models of Wood (1990). Wegner et al. obtained a mass of $M = 1.02\ M_\odot$ using the mass-radius relation of Hamada & Salpeter (1961) for carbon configurations, which indicates that finite-temperature effects are small for this object.

From the distance modulus of the Pleiades cluster, the effective temperature (with the corresponding bolometric correction), and the apparent magnitude, Wegner et al. (1991) derived a value of $\log R/R_\odot = -2.13 \pm 0.03$, which combined with the observed redshift gives directly $M = 0.98 \pm 0.17\ M_\odot$. Since this value does not depend on any mass-radius relation, it is concluded from the good agreement with the other estimate of $1.02\ M_\odot$ that the results are consistent with the mass-radius relation. Both values are also in excellent agreement with the mass obtained from spectroscopy, $M = 0.983 \pm 0.034\ M_\odot$.

Another independent test can be performed using the M_V value of LB 1497 given in Table 1. The distance modulus is obtained directly and has a value of 5.69 ± 0.10 mag, where the uncertainty has been propagated from the external errors of $T_{\rm eff}$ and $\log g$ discussed in § 3.3. This value is marginally consistent with the distance modulus of the Pleiades, 5.54 ± 0.06 mag, adopted in the analysis of Wegner et al. (1991).

6.2. *GD 50*

The highest mass at 1.27 $M_\odot$ is assigned to the star GD 50 which lies at about $\sim 5\ \sigma(M)$ above the mean mass; the next most massive object is LB 1497. GD 50 has been the subject of a detailed analysis by Bergeron et al. (1991a) though the parameters determined from this study alone differ slightly. The ultraviolet energy distribution is consistent with an effective temperature near 43,000 K. The lower temperature obtained here may result from the reduced sensitivity of the spectroscopic technique at high effective temperatures, although the independent analysis of the Lyα profile by Vennes, Thejll, & Shipman (1991) indicates a value of $T_{\rm eff} =$ 39,300 K, in good agreement with the spectroscopic temperature. If one assumes a unique relation between the initial mass and final mass, GD 50 would be an object younger than the Pleiades cluster. Since it does not appear to lie in a region of recent star formation, its origin might instead be ascribed to a merger as discussed in Bergeron et al. (1991a)—for example, a merger of components slightly more massive than those in the close binary DA system L870-2 (Saffer, Liebert, & Olszewski 1988; Bergeron et al. 1989). Two similar objects have been identified recently by Schmidt et al. (1992): PG 0136+251, previously believed to be magnetic, actually turned out to have an unusually high surface gravity of $\log g = 9.00$ ($T_{\rm eff} = 39{,}190$ K) which corresponds to a mass of 1.20 $M_\odot$. This star is listed as DA1 in McCook & Sion (1987) and hence was not part of the sample. The second object, PG 1658+441, was previously known to be magnetic and has been assigned a mass of 1.31 $M_\odot$, although for this object, the analysis is complicated by the splitting and magnetic broadening of the hydrogen line profiles in a surface field of some 2 MG.

6.3. *The Hyades White Dwarfs*

As claimed by Wegner, Reid, & McMahan (1989), the mean mass of the Hyades white dwarfs is higher than for the field white dwarfs. The first four objects (with multiple determinations) in Table 4 are members of the Hyades cluster. Since these stars have similar effective temperatures and cooling ages, they should have similar progenitor masses. However, the first gravitational redshift measurement of HZ 14 implies a mass well below the mean of the other Hyades and even of field white dwarfs. As discussed by Wegner & Reid (1991), the second measurement is more consistent with the mass-radius relation, and with the mass of other Hyades members as well. The average mass derived from spectroscopy is $M = 0.626\ M_\odot$ with a standard deviation of only 0.016 $M_\odot$. If only the second measurement of HZ 14 and an average value for GH 7-233 are considered, the mean mass obtained from gravitational redshift determinations is 0.645 $M_\odot$, with a somewhat larger scatter of 0.024 $M_\odot$. From Table 1, the distance moduli for these stars are 3.36, 3.41, 3.37, and 3.50 mag, respectively, with an average of 3.41 mag. The average is consistent with most determinations of the Hyades distance modulus (Hanson 1975).

6.4. *40 Eri B*

The spectroscopic solution achieved for 40 Eri B, $M = 0.510 \pm 0.028\ M_\odot$ (or $M = 0.526 \pm 0.026\ M_\odot$ for the second solution of Table 2), is in excellent agreement with the mass obtained from the gravitational redshift measurement of Wegner & Reid (1987; $M = 0.52 \pm 0.04\ M_\odot$). Recently, Koester & Weidemann (1991) obtained a new value of $M = 0.53 \pm 0.04\ M_\odot$, although in their analysis, the mass has been derived from the Hamada-Salpeter relation for carbon configuration, while the value given in Table 4 ($M = 0.554 \pm 0.019\ M_\odot$) has been interpolated from the evolutionary models of Wood (1990). The latter value is larger than, but still consistent with the spectroscopic determination.

Koester & Weidemann (1991) have also obtained a value of $T_{\rm eff} = 17{,}000 \pm 200$ K based on Strömgren photometry. Published values of Strömgren photometry found in the literature are certainly consistent: $(b-y), (u-b) = -0.047, +0.360$ (Graham 1972), $-0.048, +0.367$ (Wegner 1979), and $-0.051, +0.348$ (Wegner 1983). From these values and the present grid of model atmospheres, and average temperature of $T_{\rm eff} =$ 17,200 K is derived, in excellent agreement with the solution of Koester & Weidemann (1991). However, the surface gravity solution obtained from Strömgren photometry is $\log g = 7.41$, corresponding to a mass of $\sim 0.3\ M_\odot$, which is clearly at odds with all previous mass determinations. A similar conclusion is reached if the $(v-y)$ color index is used instead. The analysis of KSW based on combined Strömgren, Johnson, and MCSP color indices yields a similar solution for the effective temperature, $T_{\rm eff} = 16{,}942$ K, with a somewhat larger value of $\log g = 7.56$ (or $M = 0.38\ M_\odot$).

The determination obtained from multiple observations of 40 Eri B presented in Table 2 shows that the spectroscopic temperature is somewhat cooler than that obtained from Strömgren photometry. However, the spectroscopic solution is in excellent agreement with that achieved by WK ($T_{\rm eff} =$ 16,470 K, $\log g = 7.73$, $M = 0.45\ M_\odot$). The spectroscopic temperature is also consistent with the temperature obtained from the analysis of the Lyα profile ($T_{\rm eff} = 16{,}325 \pm 325$ K; Holberg, Wesemael, & Basile 1986), with a value of $\log g = 7.65 \pm 0.20$ which is only marginally consistent with the spectroscopic log g determination. And finally, the solution presented here is in very good agreement with the solution obtained by Schulz & Wegner (1981) based on their analysis of observed photometry and equivalent widths of Hα to Hϵ ($T_{\rm eff} = 16{,}000 \pm 1500$ K, $\log g = 7.8 \pm 0.3$).

Koester & Weidemann (1991) also discuss the inconsistency of the spectroscopic solution with that obtained from trigonometric parallax. The value used in their analysis ($\pi = 0.2084 \pm 0.0023$) is that of Gliese & Jahreiß (1987) which agrees with the value of van Altena et al. (1992) used in Table 3. These values are *not* new measurements, but represent weighted means of values published in the literature. Examination of the results presented in the McCook & Sion catalog indicate a wide range of values from 0.194 to 0.221, but only one measurement actually is consistent with the Gliese & Jahreiß weighted mean value and listed errors. From the solutions of KSW and WK, the trigonometric parallaxes are predicted to be 0.158 and 0.180, respectively, much smaller than the observed value. The value predicted from the spectroscopic solution, $\pi = 0.1959 \pm 0.0054$, is also inconsistent with the value adopted by Gliese & Jahreiß, but falls within the range of values quoted in the McCook & Sion catalog.

In order to achieve a better internal consistency with the observed trigonometric parallax, Koester & Weidemann (1991) suggest that the surface gravity of 40 Eri B obtained from spectroscopy is underestimated. Indeed, with a higher value of $\log g = 8.0$ and their photometric temperature of 17,000 K, one predicts a trigonometric parallax of $\pi = 0.2079$ which agrees perfectly with the value determined by Gliese & Jahreiß. With this solution, however, the corresponding mass of 0.59 $M_\odot$ which is uncomfortably high compared to the many previous determinations, including that obtained from the gravitational redshift measurement.

The discrepancy in the parallax discussed above has recently been removed with a modern measurement of the trigonometric parallax of the 40 Eri system obtained at the US Naval Observatory (Conard Dahn, private communication) from 32 plates covering the period 1984.7–1991.1. One may plausibly assign a higher weight to a USNO measurement than to those obtained over decades with smaller refracting telescopes. The result is $\pi = 0.1985 \pm 0.0026$, in excellent agreement with the spectroscopic prediction. The spectroscopic solution for 40 Eri B is now consistent with all the available information on that star, except with the astrometric mass of 0.43 ± 0.02 $M_\odot$ obtained by Heintz (1974). The same conclusion was reached by Koester & Weidemann (1991) where an error analysis is presented which shows that the error quoted by Heintz is likely to be underestimated.

6.5. *GD 13, GD 448, and PG 1241−010*

Zuckerman & Becklin (1992) have recently published a survey aimed at discovering low-luminosity nondegenerate companions to white dwarf stars. Their technique consists of searching for infrared excesses in white dwarf energy distributions. They have surveyed 200 white dwarf stars, of which 21 have cool companions within 6″ of the white dwarf. Three of these objects are in common with the present analysis: GD 13, GD 448, and PG 1241−010. Quite remarkably, the last two objects have inferred masses of $M = 0.35$ and 0.31 $M_\odot$, respectively. As discussed earlier, such low masses imply that these stars must have undergone prior phases of common envelope evolution in close binary systems.

The third object, GD 13, has a higher mass of $M = 0.50$ $M_\odot$. Note that the distance modulus obtained here, 4.59 mag, differs significantly from the value given in Table 1 of Zuckerman & Becklin (1992), 3.92 mag, which has been derived from relations between photometry and absolute visual magnitude such as those given in McCook & Sion (1987). This distance moduli of the other two objects have been obtained from the results presented in Table 1.

7. CONCLUSIONS

The spectroscopic method of determining atmospheric parameters has been applied to a magnitude-limited sample of 129 DA stars with effective temperatures above $T_{\rm eff} \sim 14{,}000$ K. The masses have been inferred from detailed evolutionary sequences which show that finite-temperature effects are important for such analyses. The technique has been shown to be easily applicable to a large number of stars with high accuracy, especially in a relative sense. A mean mass of 0.562 $M_\odot$ has been derived for the complete sample, but there is an uncertain correction from a magnitude-limited to a volume-complete sample. The median or mode values are more useful statistics: The distribution peaks at lower mass, in the range 0.50–0.55 $M_\odot$ where about a third of the stars are found (the median has a value of $M = 0.540$ $M_\odot$). This differs somewhat from the findings of WK where a similar fraction of their sample is found in a range of masses twice as large. Therefore, the mass distribution has an even narrower peak than they previously argued. The mean mass obtained in the best previous analyses is somewhat higher than estimated here. However, KSW have shown that a lower mean mass can be obtained when their analysis is restricted to a range of temperature hotter than $T_{\rm eff} = 13{,}000$ K. This is also the range of temperature where atmospheric convection in DA stars becomes negligible.

As mentioned in § 1.3, the motivation behind the investigation is to avoid the uncertainties related to the atmospheric composition and to the modeling of convection in the atmospheres of cooler white dwarfs. Therefore, the results presented here provide an estimate of the mass distribution for DA stars which is independent of these particular theoretical uncertainties. Most previous investigations, and especially that of WK, were concentrated on stars whose atmospheres are convective and where model atmospheres are sensitive to the assumed convective efficiency ($T_{\rm eff} \sim 8000$–15,000 K). In the light of the analysis of Bergeron et al. (1992), the lower mean mass found here could imply that convection is more efficient than previously anticipated. Indeed, it was demonstrated that the morphology of color-color diagrams is very sensitive to the treatment of convection: had a more efficient convection been used in previous photometric analyses, the mean surface gravity of DA white dwarfs in this range of effective temperatures would have been found to be lower than the canonical $\log g = 8.0$ value (see Figure 2 of Bergeron et al. 1992).

The results derived in this investigation can ultimately be used to *calibrate* the mixing-length theory in the atmospheres of DA stars by assuming an extension of the same mass distribution into the cooler convection-dependent temperature range. Such an analysis is currently underway, the results of which will be reported elsewhere.

We are grateful to M. A. Wood, C. C. Dahn, S. K. Leggett, W. F. van Altena, T. Schöning, and K. Butler for providing us with unpublished material for this investigation, and to J. B. Holberg, K. M. Kidder, B. Zuckerman, D. G. Hummer, and M. J. Seaton for enlightening discussions. This work was supported in part by the NSF grant AST 91-45162, by the NSERC Canada, and by the Fund FCAR (Québec). P. B. acknowledges support from a NSERC postdoctoral fellowship.

REFERENCES

Baschek, B., & Norris, J. 1975, ApJ, 199, 695
Bergeron, P., Kidder, K. M., Holberg, J. B., Liebert, J., Wesemael, F., & Saffer, R. A. 1991a, ApJ, 372, 267
Bergeron, P., Saffer, R. A., & Liebert, J. 1991b, in Confrontation between Stellar Pulsation and Evolution, ed. C. Cacciari, & G. Clementini (ASP Conf. Ser., 11), 513
———. 1991c, in 7th European Workshop on White Dwarfs, ed. G. Vauclair & E. M. Sion (NATO ASI Series), 75
Bergeron, P., Wesemael, F., & Fontaine, G. 1991d, ApJ, 367, 253
———. 1992, ApJ, 387, 288
Bergeron, P., Wesemael, F., Fontaine, G., & Liebert, J. 1990, ApJ, 351, L21
Bergeron, P., Wesemael, F., Liebert, J., & Fontaine, G. 1989, ApJ, 345, L91
Bragaglia, A., Greggio, L., Renzini, A., & D'Odorico, S. 1990, ApJ, 365, L13
Daou, D., Wesemael, F., Bergeron, P., Fontaine, G., & Holberg, J. B. 1990, ApJ, 364, 242
Demers, S., Fontaine, G., Wesemael, F., Lamontagne, R., & Irwin, M. J. 1987, in IAU Colloq. 95, The Second Conference on Faint Blue Stars, ed. A. G. Davis Philip, D. S. Hayes, & J. Liebert (Schenectady: L. Davis), 497
Dolez, N., Vauclair, G., & Koester, D. 1991, in 7th European Workshop on White Dwarfs, ed. G. Vauclair & E. M. Sion (NATO ASI Series), 361

Downes, R. 1986, ApJS, 61, 569
Fontaine, G., Bergeron, P., Lacombe, P., Lamontagne, R., & Talon, A. 1985, AJ, 90, 1094
Fontaine, G., Bergeron, P., Vauclair, G., Brassard, P., Wesemael, F., Kawaler, S. D., Grauer, A. D., & Winget, D. E. 1991, ApJ, 378, L49
Fontaine, G., Tassoul, M., & Wesemael, F. 1984, in Proc. 25th Liège Astrophysical Colloquium: Theoretical Problems in Stellar Stability and Oscillations, ed. A. Noels & M. Gabriel (Liège: Universitè de Liège), 328
Fontaine, G., & Wesemael, F. 1987, in IAU Colloq. 95, The Second Conference on Faint Blue Stars, ed. A. G. D. Phillip, D. S. Hayes, & J. Liebert (Schenectady: L. Davis), 319
Foss, D., Wade, R. A., & Green, R. F. 1991, ApJ, 374, 281
Gatewood, G. D., & Gatewood, C. V. 1978, ApJ, 225, 191
Gliese, W., & Jahreiß, H. 1987, Catalog of Nearby Stars (3d ed.; in preparation), as cited in McCook & Sion 1987
Graham, J. A. 1972, AJ, 77, 144
Green, R. F., Schmidt, M., & Liebert, J. 1986, ApJS, 61, 305
Greenstein, J. L. 1984, ApJ, 276, 602
Greenstein, J. L., & Sargent, A. 1974, ApJS, 28, 157
Hamada, T., & Salpeter, E. E. 1961, ApJ, 134, 683
Hanson, R. B. 1975, AJ, 80, 379
Hayes, D. S., & Latham, D. W. 1975, ApJ, 197, 593
Heintz, W. D. 1974, AJ, 79, 819
Holberg, J. B., Wesemael, F., & Basile, J. 1986, ApJ, 306, 629
Hummer, D. G., & Mihalas, D. 1988, ApJ, 331, 794
Iben, I., Jr. 1990, ApJ, 353, 215
Iben, I., Jr., & Tutukov, A. V. 1987, ApJ, 311, 742
Kawaler, S. D. 1991, in Confrontation between Stellar Pulsation and Evolution, ed. C. Cacciari & G. Clementini (ASP Conf. Ser., 11), 494
Koester, D. 1984, Ap&SS, 100, 471
———. 1987, ApJ, 322, 852
Koester, D., Schulz, H., & Weidemann, V. 1979, A&A, 76, 262 (KSW)
Koester, D., & Weidemann, V. 1980, A&A, 81, 145
———. 1991, AJ, 102, 1152
Lanning, H., & Pesch, P. 1981, ApJ, 244, 280
McCook, G. P., & Sion, E. M. 1987, ApJS, 65, 603
McMahan, R. K. 1989, ApJ, 336, 409
Oke, J. B., & Gunn, J. E. 1983, ApJ, 266, 713
Press, W. H., Flannery, B. P., Teukolsky, S. A., & Vetterling, W. T. 1986, Numerical Recipes (Cambridge: Cambridge Univ. Press)
Saffer, R. A., Bergeron, P., Koester, D., & Liebert, J. 1992, in preparation
Saffer, R. A., Liebert, J., & Green, R. F. 1992, in preparation
Saffer, R. A., Liebert, J., & Olszewski, E. M. 1988, ApJ, 334, 947
Schmidt, G. D., Bergeron, P., Liebert, J., & Saffer, R. A. 1992, ApJ, in press
Schulz, H., & Wegner, G. 1981, A&A, 94, 272
Seaton, M. J. 1990 J. Phys. B, 23, 3255
Shipman, H. L. 1979, ApJ, 228, 240
Shipman, H. L., & Sass, C. A. 1980, ApJ, 235, 177
Tüg, H., White, N. M., & Lockwood, G. W. 1977, A&A, 61, 679
Tutukov, A. V., & Yungelson, L. 1987, in IAU Colloq. 95, The Second Conference on Faint Blue Stars, ed. A. G. Davis Philip, D. S. Hayes, & J. Liebert (Schenectady: L. Davis), 435
van Altena, W. F., Lee, J. T., & Hoffleit, D. 1992, Yale General Catalog of Trigonometric Stellar Parallaxes, in preparation
Vennes, S., Thejll, P., & Shipman, H. L. 1991, in 7th European Workshop on White Dwarfs, ed. G. Vauclair & E. M. Sion (NATO ASI Series), 235
Vidal, C. R., Cooper, J., & Smith, E. W. 1970, ApJS, 25, 37
Wegner, G. 1979, A&A, 84, 1384
———. 1983, A&A, 88, 109
———. 1989, in IAU Colloq. 114, White Dwarfs, ed. G. Wegner (New York: Springer), 401
Wegner, G., & Reid, I. N. 1987, in IAU Colloq. 95, The Second Conference on Faint Blue Stars, ed. A. G. Davis Philip, D. S. Hayes, & J. Liebert (Schenectady: L. Davis), 649
———. 1991, ApJ, 375, 674
Wegner, G., Reid, I. N., & McMahan, R. K. 1989, in IAU Colloq. 114, White Dwarfs, ed. G. Wegner (New York: Springer), 378
———. 1991, ApJ, 376, 186
Wegner, G., & Schulz, H. 1981, A&AS, 43, 473
Weidemann, V., & Koester, D. 1983, A&A, 121, 77
———. 1984, A&A, 132, 195 (WK)
Wesemael, F., Auer, L. H., Van Horn, H. M., & Savedoff, M. P. 1980, ApJS, 43, 159
Wesemael, F., Bergeron, P., Fontaine, G., & Lamontagne, R. 1991, in 7th European Workshop on White Dwarfs, ed. G. Vauclair & E. M. Sion (NATO ASI Series), 159
Winget, D. E., et al. 1991, ApJ, 378, 326
Wood, M. A. 1990, Ph.D. thesis, University of Texas at Austin
Wood, M. A., & Bergeron, P. 1992, in preparation
Yuan, J. W. 1989, A&A, 224, 108
Zuckerman, B., & Becklin, E. E. 1992, ApJ, 386, 260